

A Monte Carlo approach to the inverse problem of diffuse pollution risk in agricultural catchments

David G. Milledge, Stuart N. Lane, A. Louise Heathwaite and Sim M. Reaney

Abstract

The hydrological and biogeochemical processes that operate in catchments influence the ecological quality of freshwater systems through delivery of fine sediment, nutrients and organic matter. Most models that seek to characterise the delivery of diffuse pollutants from land to water are reductionist. The multitude of processes that are parameterised in such models to ensure generic applicability make them complex and difficult to test on available data. Here, we outline an alternative – data-driven – inverse approach. We apply SCIMAP, a parsimonious risk based model that has an explicit treatment of hydrological connectivity. We take a Bayesian approach to the inverse problem of determining the risk that must be assigned to different land uses in a catchment in order to explain the spatial patterns of measured in-stream nutrient concentrations. We apply the model to identify the key sources of nitrogen (N) and phosphorus (P) diffuse pollution risk in eleven UK catchments covering a range of landscapes. The model results show that: 1) some land use generates a consistently high or low risk of diffuse nutrient pollution; but 2) the risks associated with different land uses vary both between catchments and between P and N delivery; and 3) that the dominant sources of P and N risk in the catchment are often a function of the spatial configuration of land uses. Taken on a case by case basis, this type of inverse approach may be used to help prioritise the focus of interventions to reduce diffuse pollution risk for freshwater ecosystems.

Keywords: Diffuse pollution; Hydrological connectivity; Land cover; Nutrients; Nitrogen; Phosphorus; Risk; Modelling.

1. Introduction

The source-mobilisation-delivery conceptualisation of diffuse pollution transfer from land to water is widely accepted (Heathwaite, 2010) and forms the basis of several existing diffuse pollution models that seek to explain the variation in river water quality over time in terms of the processes and pathways of delivery operating within a catchment. Much effort has been focused on characterising the variation in water quality timeseries (Burt *et al.*, 2011; Howden *et al.*, 2010; Kirchner *et al.*, 2004; Neal *et al.*, 2010a)

31 or producing a good fit between modelled processes and measured water quality (Lazar *et al.*, 2010;
32 Whitehead *et al.*, 2007) but such effort does not elucidate the spatial signals in a catchment. Not all
33 locations in a river catchment (even if they have the same land use) contribute equally to the delivery of
34 sediment or nutrients and hence to in-stream sedimentation and water quality degradation (Heathwaite
35 *et al.*, 2000; Lane, 2008; Page *et al.*, 2005; Pionke *et al.*, 2000). Critical source areas (CSAs) in
36 catchments are characterised by the capacity to entrain material and to connect and hence deliver it to
37 the drainage network (Sharpley *et al.*, 2008; 2009). The environmental degradation associated with
38 diffuse nutrient and sediment losses from land to water may be redefined as comprising a series of
39 spatially-distributed sources of varying size (often fields, or even parts of fields) where particularly risky
40 uses of land combine with a high probability of connection of those risks to the river network (Heathwaite
41 *et al.*, 2000; Lane *et al.*, 2006; Lane 2008). Focusing intervention measures on reducing diffuse pollution
42 delivery from these risky land uses should maximise the return on investment in terms of improvements
43 to ecological quality (Collins and McGonigle, 2008; Heathwaite, 2010; Living With Environmental
44 Change, 2011).

45 A range of modelling approaches have been developed to meet the challenge of identifying the locations
46 within a catchment that have the greatest probability of contributing high diffuse pollution loads to
47 receiving waters. Lane *et al.* (2006) classify diffuse pollution models into three main groups: (1) transfer
48 function modelling – which predicts nutrient export on the basis of simple empirical transfer functions
49 driven by known fertiliser and manure inputs coupled with soil nutrient status (e.g., Ekholm *et al.*, 2005;
50 Heathwaite *et al.*, 2003a; Johnes, 1996; Johnes *et al.*, 2007; Jordan *et al.*, 1994; Khadam and
51 Kaluarachchi, 2006); (2) land unit modelling – which applies physically-based (sometimes called
52 mechanistic) models of nutrient cycling to individual land units in order to determine export (e.g.
53 Matthews, 2006; Priess *et al.*, 2001; Vatn *et al.*, 2006); (3) land transfer modelling – which combines the
54 kind of analysis described in (2) with a physically-based, sometimes dynamic, treatment of how material
55 is transferred across the landscape (e.g. Easton *et al.*, 2008; Neumann *et al.*, 2010; Wade *et al.*, 2002).
56 The latter (see Radcliffe *et al.*, 2009) ought to capture effectively the delivery of diffuse pollutants. The
57 main difficulty is whilst they are physically-based they contain parameters or require data whose values
58 either: (i) cannot be determined from available data; or (ii) need to be adjusted, calibrated, so as to force
59 the model to fit known system response (Oreskes *et al.*, 1994). The information demanded in terms of
60 data and model parameters may exceed the information content of calibration data (Heathwaite, 2003;

61 2010; Kirchner, 2006) and different model realisations (i.e. model runs with different parameter
62 combinations) may have very similar levels of success (i.e. equifinality, Beven, 1993).

63 Mathematical models are constructed through a process where, in response to a perception of what
64 matters to the system of interest, the processes that need to be modelled are identified (e.g. rainfall,
65 evapotranspiration, infiltration, runoff generation, biogeochemical processing, mobilisation of material
66 into solution and its subsequent transformation in transit, etc). A suitable model to represent these
67 processes will then be identified, modified or developed. This process is implicitly reductionist and points
68 to the development of ever more complex models given the multitude of processes that could be
69 included to guarantee that the model can be applied in many situations. There are two responses to this
70 challenge. The first couples conventional predictive models with differing levels of process complexity at
71 different scales (e.g. Hewett *et al.*, 2009; Quinn, 2004). Each level contains process complexity that is
72 appropriate to the information available to that scale of enquiry. Information is then exchanged between
73 scales as a means of scaling up. The second, which we focus on here, uses a risk-based analysis with a
74 single simplified model to represent all scale ranges. These approaches have proved very effective in
75 diffuse pollution modelling (e.g. Heathwaite *et al.*, 2003a, b; Johnes and Heathwaite, 1997; Jordan *et al.*,
76 1994; Munafo *et al.*, 2005; Siber *et al.*, 2009; Weld and Sharpley, 2007). Their primary assumption is
77 that the amount of material that is exported from a land unit can be traced to the properties of that land
78 unit (e.g. physical attributes like slope and soil type) and how it is managed (e.g. levels of fertiliser
79 application). Measurements have allowed identification of associated export coefficients, which in many
80 cases have some kind of *a priori* or logical basis (e.g. export coefficients for a pollutant that is eroded
81 whilst bound to fine sediment are greater for land uses where vegetation cover is bare for part of the
82 year). We label this 'forward modelling'.

83 This paper presents an alternative conceptualisation, in which we consider the problem and use a
84 Bayesian approach to determine the weightings that must be given to different land uses in order to
85 explain spatial patterns of measured in-stream nutrient concentrations. Following Mosegaard and
86 Tarantola (2002), inverse modelling involves using a physical theory (or set of theories) to connect a set
87 of model parameters to a set of observations. In an inverse model, the forward model is inverted so as to
88 predict the model parameters that reproduce those observations. In some cases this inversion is
89 tractable using maximum likelihood methods but not in all cases (Mosegaard and Tarantola, 2002). The
90 inverse problem can also be approached by pseudo-randomly generating a large collection of (forward)

91 models, then analyzing and displaying the models to convey information on the relative likelihoods of
92 model properties (Mosegaard and Tarantola, 1995). This can be accomplished using a Monte Carlo
93 method even in cases where no explicit formula for the a priori distribution is available (Mosegaard and
94 Tarantola, 1995). It is this latter approach that we adopt here, with the objective of making as few *a priori*
95 assumptions as possible about what might be driving river water quality patterns (Lane 2008).

96 Following observations regarding critical source areas, we retain the assumption that locations will vary
97 spatially in their ability to generate and deliver diffuse pollution risk. It is clear that in trying to understand
98 the relative contribution of diffuse pollutants in catchments, model assumptions have a material impact
99 upon the way a system is modelled (e.g. the assumed contribution of point and diffuse pollution sources
100 will fundamentally impact upon the extent to which a model must focus upon point source delivery of
101 discharges from sewage treatment plants and urban drainage). By taking an inverse approach, we ‘train’
102 each model to the local characteristics of each catchment, avoiding the need for a generic model in
103 which many model parameters may end up being superfluous and where training (or calibration) is
104 difficult because there is rarely enough data to distinguish between different model formulations (Beven,
105 1989). The aim of this paper is to present our approach to the inverse problem for two key nutrients
106 associated with diffuse pollution: phosphorus (P) and nitrogen (N). Both nutrients are particularly
107 important controls on the ecological quality of freshwater systems (Heathwaite, 2010). We use the
108 results of our analysis to show that policy interventions designed to reduce the risk of diffuse pollution
109 need to be sensitive to the relationship between nutrients, relative land use dominance and catchment
110 characteristics, including land use configuration and hydrological properties.

111

112 **2. Methods**

113 ***2.1. The SCIMAP model***

114 We use SCIMAP to produce a risk-based estimation of diffuse pollution (see Lane *et al.*, 2006 and
115 Reaney *et al.*, 2011) and a full description is provided in the Supplementary Online Material that
116 accompanies this manuscript (Appendix 1). SCIMAP conceptualises catchments as comprising a
117 collection of flow paths that accumulate spatially distributed sources that may result in the pollution of
118 receiving waters from across the landscape and deliver them into the river corridor. It is within the river

119 corridor that diffuse pollution may become 'visible', either through detection of temporal changes in water
120 quality via routine monitoring (e.g. elevated nitrate concentrations) or through the more limited, evidence
121 from physical water quality deterioration (e.g. algal blooms, Hilton et al., 2006; or long-term changes in
122 ecological quality, Reaney et al., 2011). Given an observed change in catchment water quality a primary
123 challenge is to attribute this to its sources, whether point source or diffuse. If the latter, the challenge
124 becomes over which locations are likely to be the significant CSAs. SCIMAP's approach is relative in
125 that, subject to data availability, the model can be applied at any scale, with the predictions relative to the
126 scale at which the model is used. It allows successive identification (in relative terms) of the catchments
127 that merit prioritisation, followed by the sub-catchments and then eventually the associated fields. A full
128 description and application of the model is provided in Reaney *et al.* (2011) who show how SCIMAP can
129 be used to understand the relationships between land use, hydrological connectivity and the spatial
130 distributions of salmonid populations. In this paper, we use an inverse approach to estimate the
131 generation risk by inferring how land uses need to be weighted to optimise the explanation of spatial
132 patterns of measured water quality parameters. We use an informal Bayesian likelihood estimation
133 procedure conceptually similar to the Generalised Likelihood Uncertainty Estimation approach (Beven
134 and Binley, 1992; Vrugt *et al.*, 2009).. We use water quality data that are available through the
135 Environment Agency for England and Wales (EA) General Quality Assessment (GQA) monitoring
136 network (see: <http://bit.ly/EA-GQA>). These datasets are described in more detail later in the paper.

137

138 **2.2. Application**

139 The SCIMAP model framework has five general steps; the focus of the inverse approach reported in this
140 paper is Step (1), which is described in full below. Further detail of Steps (2) to (5) and full justification is
141 given in Reaney *et al.* (2011) and in the Supplementary Online Material (Appendix 1); only a brief
142 summary is given here. Step (1) seeks to identify, in relative terms and for each location in a landscape,
143 the risks of diffuse pollution generation. Step (2) determines the risk of delivery, the delivery index, for
144 each location. This is based upon the assumption that the driest point along a flow path between a
145 location, *i*, and the river is the one that is most likely to control the extent to which material moving over
146 the surface or the shallow subsurface moves vertically as opposed to laterally and, in so doing, becomes
147 hydrologically-disconnected from the surface water system. Lane *et al.* (2009) show that using this

148 measure to determine a delivery index can explain a significant proportion of the tendency towards
149 hydrological connection. We derive the delivery index from 10 m resolution digital elevation models
150 collected using airborne Interferometric Synthetic Aperture Radar (see Reaney *et al.* 2011). We
151 emphasise that the analysis makes a specific assumption that topography exerts a primary control on
152 the spatial structure of soil moisture in agricultural catchments. Each location then has a risk of diffuse
153 pollution generation and a risk of delivery. These are scaled to give relative generation and delivery risks
154 for each location in the catchment and multiplied together (Step 3). In Step 4, the resultant location risks
155 are routed through the catchment to the river network, using the same topographic data used in Step 2.
156 Step 4 results in a monotonically increasing level of risk with distance downstream in the river network
157 and so in Step 5 we correct this by dividing the result by the upslope contributing precipitation for each
158 location in the river network, using annual average precipitation data, based on the UKCP09 baseline
159 (Perry and Hollis, 2005).

160

161 **2.2.1. Generation Risk**

162 In this paper, we use a sampling approach to the inverse problem in Step (1). Step (1) is underpinned by
163 the assumption that some land use and/or land management combinations are more likely to generate
164 diffuse pollution risk than others, and we can use land cover as a first approximation of this risk. There
165 are well-established approaches for determining the risk of diffuse pollution generation from land cover,
166 ranging from the simpler export coefficient models (e.g. Heathwaite *et al.*, 2003a; Johnes, 1996) through
167 to more complex models of sediment entrainment and nutrient cycling (e.g. Vatn *et al.*, 2006). Here, we
168 use an informal Bayesian inference methodology to infer the risk weighting that needs to be given to
169 each land cover in order to optimise a spatially-distributed set of water quality observations. Our analysis
170 is focused on P and N risk as two of the key consequences of agricultural diffuse pollution and drivers of
171 the deterioration of ecological quality in freshwaters. Here, we assume that: different land covers
172 generate different diffuse pollution risks; within land cover risk variability is small relative to that between
173 land covers; and the pattern of land covers is fixed over the observation period. The aim of Step (1) is
174 then to infer the optimum land cover risk weighting in the SCIMAP framework, so as to maximise the
175 level of explanation in a spatially-variable, measured, risk indicator.

176

177 2.2.2. Land cover

178 Our starting point for Step 1, the estimation of the generation risk, is identification of land cover classes
179 from the UK Land Cover Map 2000, a digital map derived from a computer classification of satellite
180 scenes obtained mainly from Landsat satellites and with a resolution of 25 m (Fuller *et al.*, 2002). We
181 use the data in raster format (converted from the original vector database) resampled to the same
182 resolution as the elevation data (10 m) using a nearest neighbour algorithm. These data represent the
183 finest resolution and most precise UK wide land cover dataset that was available at the time of analysis.
184 The Foresight Land Use Futures Report (2010) highlighted the difficulties in obtaining accurate and
185 current land use data for the UK, partly as a result of the way the data is collected but also because
186 synthesising very different data sources to produce a UK land use map remains a challenge. The Land
187 Cover Map records 16 classes and 27 subclasses within the 'Broad Habitats' classification (Jackson,
188 2000). We grouped these broad habitats and their subcomponents into ten land cover classes that have
189 potential to contribute varying magnitudes of diffuse pollutants to receiving waters. The ten classes
190 chosen with respect to their likely linkage to diffuse pollution sources are: improved grassland, rough
191 grass, moorland, bog, urban, cereals, horticulture, non-rotational horticulture, woodland, and 'other',
192 which was set to represent those land covers (e.g. lakes) with zero risk. Table 1 gives the relationship
193 between the broad habitat classes and the ten SCIMAP classes. Improved grassland is regularly re-
194 seeded and receives significant nutrient inputs usually as slurry and/or fertiliser; the dominance of
195 palatable grasses gives these areas a distinct spectral signature (Fuller *et al.*, 2002). Rough grass land
196 covers are dominated by very low productivity grasses, they are not normally improved by reseeded or
197 fertilizer applications because the land tends to be physically-limiting (e.g. too wet, too steep, too rocky)
198 and can include areas dominated by *Pteridium aquilinum* at the height of the growing season. Moorland
199 cover is characterised by large expanses (> 25%) of ericaceous species and gorse. Bogs are either
200 upland or lowland areas that are permanently, seasonally or periodically waterlogged defined based on
201 both vegetation (ericaceous, herbaceous and mossy swards) and peat depth (> 0.5 m from peat drift
202 maps). Urban land covers range from single buildings to large towns or cities and include: roads, derelict
203 ground, and gardens. Cereals include spring and winter crops; horticulture includes arable bare ground
204 and non-cereal spring crops; and non-rotational horticulture includes orchards and non-grass setaside.
205 Woodland includes both broad-leaved and coniferous woodland.

206 <Table 1 near here>

207

208 **2.2.3. Risk indicator**

209 The inverse approach requires time-integrated, spatially-distributed datasets that can provide an
210 indication of water quality. Here, we use the General Quality Assessment (GQA) data collected by the
211 EA, which has over 7000 observation sites across England and Wales. The EA GQA scheme does not
212 routinely determine total P. Most samples are analyses for the inorganic dissolved P fraction with P
213 determined as orthophosphate on *unfiltered* water samples with a limit of detection of $0.0082 \text{ mg l}^{-1} \text{ PO}_4^{3-}$
214 -P and a reporting limit of $< 0.02 \text{ mg l}^{-1} \text{ PO}_4^{3-}\text{-P}$. Like P, total N is not routinely analysed in the GQA
215 scheme. The most robust data are records of nitrogen as nitrate (NO_3^- -N) for unfiltered water samples
216 calculated by the difference between Total Oxidised Nitrogen (TON) and NO_2^- -N. The limit of detection is
217 $0.0294 \text{ mg l}^{-1} \text{ NO}_3^-$ -N and the reporting limit is $< 0.2 \text{ mg l}^{-1} \text{ NO}_3^-$ -N.

218 The viability of the GQA dataset for our application is governed by the spatial distribution of the
219 observations. The GQA sample locations are not chosen exclusively to monitor the impact of diffuse
220 pollution on water quality; legislative drivers are particularly important (e.g. monitoring point source
221 discharges and water abstraction). Consequently, there is some bias towards sampling sites above and
222 below point sources such as sewage treatment works. Here, we take advantage of this bias: rather than
223 excluding urban land cover from the analysis and taking measured nutrient concentrations and trying to
224 apportion them into 'point' and 'non-point' sources, we use inference (see below) to work out the
225 required risk weighting, and hence indicate the relative importance of 'urban' and 'non-urban' sources to
226 explaining spatial patterns of water quality. Thus, a catchment where urban land covers are inferred to
227 need a high weighting will be one where the spatial structure of measured water quality is influenced
228 strongly by pollution associated with urban sources rather than agricultural sources (Davies and Neal,
229 2007). The inference works on the assumption that the location of a sewage works is approximated by
230 the flow paths identified through an urban setting. Whilst urban drainage is commonly gravity driven,
231 urban drainage is complex and hence there is a possibility for error arising from deviation between the
232 flow paths inferred from topographic data in urban areas and the actual areas of the landscape (i.e.
233 urban drainage) that contribute to a sewage works.

234 The GQA scheme is designed to collect one sample per month and data were available for a 15 year
235 period, 1990-2005, with a mean of 155 observations per site. Following Davies and Neal (2007) and

236 Rothwell *et al.*, (2010a), and given that the analysis is at the scale of England and Wales we use the
237 arithmetic mean rather than flow weighted GQA concentrations from each site. This allows us to take
238 advantage of the large number of available sites that are critical to our approach, despite the lack of flow
239 data with which to develop rating curves at these sites. The highly episodic nature of nutrient transport
240 within rivers (Burt *et al.*, 2011; Doyle, 2005; Edwards and Withers, 2008; Walling and Webb, 1985),
241 suggests that the lack of flow weighting may introduce error in the mean concentration estimates
242 (Johnes, 2007) and although our own tests suggest that the number of concentrations samples is large
243 enough to capture the range of observed discharges (see Appendix 2), the results should be considered
244 in the light of this limitation. However, our approach is more robust to this measurement error than
245 others, since the relative rather than absolute magnitude of the concentrations is more important in a risk
246 based framework.

247

248 **2.2.4. Inference of land cover risk weightings**

249 The inference of land cover risk weightings used a Monte Carlo sampling framework. We undertook
250 5,000 model simulations, randomly selecting weightings in the range 0 to 1 for each land cover for each
251 simulation (see Appendix 3 in the Supplementary Online Material for details on our choice of 5000
252 simulations). No *a priori* likelihood is assigned to these weightings. For each simulation, an objective
253 function is determined, in this case a correlation coefficient, that describes the level of association
254 between the water quality indicator (the spatially-distributed, mean GQA P and N concentrations) and
255 their spatially-corresponding risk estimates.

256 In philosophical terms, our approach mirrors that adopted in Generalized Likelihood Uncertainty
257 Estimation and recognised in associated problems of equifinality in hydrological models (Beven and
258 Binley, 1992; Beven 1993). Equifinality refers to a situation where different combinations of model
259 parameters can result in the same or similar model predictions. Most commonly, it is identified when
260 model predictions are compared to independent measurements, and those measurements cannot
261 distinguish between different model realisations. Our null hypothesis is that there is no systematic
262 variation in model performance between model realisations as a function of the values of a given land
263 use weighting. If we can reject the null hypothesis for a given land use, we can infer that a particular land
264 use weighting influences model performance and therefore influences instream nutrient concentrations.

265 If we accept the null hypothesis for a land use then the influence of its weighting on model performance
266 and therefore instream nutrient concentrations cannot be identified.

267 We suggest four possible reasons why the null hypothesis might be true and these are both
268 methodological and substantive. First, it may be because a given land use has little or no coverage in a
269 catchment. The inverse approach uses the influence of the land use on observations to define its risk so
270 a land use must be present in order to exert an influence. If the influence is subtle and the coverage is
271 limited the signal from this land use will be very weak. Second, high risk weightings for one land cover
272 may offset low risk weightings in another such that optimum performances can be attained with a range
273 of weightings for these land covers. This situation arises when the fraction of the landscape in a given
274 land cover class (weighted by the average delivery index for that class) for each of the water quality
275 measurement points covaries with one or more other landscape fractions. To some extent, this is a
276 function of the available water quality data: i.e. the equifinality will become less severe with more
277 measuring points, if the fractions become progressively more differentiated. However, if present, we
278 cannot resolve this problem without additional data that avoid the covariance problem. Third, a land use
279 class may be too broad to have a single coherent weighting if it encompasses a range of management
280 practices and therefore of nutrient availability. Fourth, the model may not represent processes that are
281 important in explaining the variability in observed nutrient concentrations (e.g. instream uptake). This
282 problem is inherent to all models since they necessarily simplify the system; it tempts the developer
283 toward ever more complex models, as discussed above. One way of establishing the model's suitability
284 may be its ability to explain the variance in the observations.

285 The inverse approach provides information on three properties: identifiability, influence and importance.
286 The identifiability of a particular land cover weighting defines the extent to which we can identify an
287 optimum risk weighting given the uncertainty associated with those individual model realisations that give
288 the best results. We use here the standard deviation of the risk weighting for those best results and
289 where this is lower, we can conclude that the risk weighting is more identifiable. If the risk weighting is
290 more identifiable, we conclude that it has a greater influence over the model's performance than where it
291 is less identifiable. However, the link between identifiability and influence can be disrupted by equifinality
292 so that while we can infer influence from an identifiable weight, we cannot infer a lack of influence from a
293 less identifiable weight.

294 The importance of a particular land cover for instream nutrient concentrations is then defined by its risk
295 weighting (assuming that the model representation is suitable and the weighting identification is without
296 error). Land covers with below average weightings (0.5) will lower (or dilute) the diffuse pollution risk
297 whereas those with above average weightings will increase the risk. For weightings less than 0.5, the
298 land cover is a 'diluter' of the diffuse pollution signal with increasing importance as the risk tends to zero.
299 For weightings greater than 0.5, the land cover is a contributor to the diffuse pollution signal with
300 increasing importance as the risk tends to one. Identifiability remains relevant here since it informs the
301 degree of certainty with which the weighting can be identified. Errors in model structure (e.g. process
302 representation) will affect the extent to which the identified weightings reflect true risk associated with a
303 given land cover but are not represented within the identifiability since these errors can disrupt
304 identifiability or alter identified weightings (e.g. by inflating a land cover's risk weighting to account for
305 more efficient delivery).

306 To visualise the relationship between model realisations and model parameters, we plot land cover risk
307 weighting against objective function to create 'dotty plots' (Figure 1a). These plots contain considerable
308 scatter as a result of parameter interactions. For example, if the best objective function value is
309 associated with a risk weighting of 0.8 for improved grassland, not all simulations with the improved
310 grassland weighting close to 0.8 will produce good objective function values as the full set of simulations
311 are considered, within which the weightings assigned to other land covers will not be optimal. However,
312 pattern in the scatter (e.g. trend) suggests that the improved grassland weighting exerts an influence on
313 the model's performance and the form of this trend gives some indication as to the range of reasonable
314 weightings that might be assigned to that land cover class. In the illustrative example, Figure 1a shows
315 that simulations with a high weighting for improved grassland are more likely to generate high
316 correlations with the water quality data being used to judge each simulation. The plots also identify rough
317 grass, horticulture and urban land covers as influential with rough grass and horticulture requiring a low
318 risk weighting and urban areas a weighting of ~ 0.4 . The other land covers show no clear pattern in their
319 dotty plots, and therefore we are unable to identify their influence on the models performance or their
320 importance as a source of nutrients in this catchment. As discussed above, not all land covers will
321 necessarily have identifiable weightings, especially since some land covers are absent in some
322 catchments (e.g. non-rotational horticulture in Figure 1a) and are included only to maintain a consistent
323 approach across the catchments.

324 The cloud of points in the dotty plots is not uniformly dense. We convert the dotty plots into two
325 dimensional probability density functions (pdfs) using non-overlapping bins of length 0.05 in x and y.
326 These pdfs (Figure 1b) show the probability of achieving a given value of the objective function
327 conditional on a particular risk weighting for the land cover class in question, and assuming a random
328 attribution of weightings for all the other land cover classes. This allows us to understand the relationship
329 between risk weighting and model performance better than if we look only at the trend in the upper or
330 lower limits to the dotty plot, or view the cloudiness as an indication that land cover effects cannot be
331 resolved.

332 Ranking each simulation by its correlation coefficient gives a ranked simulation list that is a measure of
333 the likelihood of each simulation having the most correct set of weightings. Starting with the x most likely
334 simulations, we determine the mean and standard deviation of the risk weightings associated with those
335 x simulations, then progressively increase x; each time recalculating the mean and the standard
336 deviation. The minimum value of x considered was 0.5% of the total number of simulations (25
337 simulations in this application) to enable stable calculations of means and standard deviations (after
338 testing their stability for $x = 5 : 100$ for a single catchment). The plot of mean and standard deviation of
339 weighting against correlation, which we term an 'optimisation plot' (Figure 1c) shows: (1) the land covers
340 with clearly identifiable risk weightings, characterised by a narrow range of weightings, or a small
341 standard deviation; and (2) the magnitude of the weighting associated with a given correlation, which
342 determines the importance of a land cover in contributing high (weightings closer to one, diffuse pollution
343 sources) or low levels of risk (weightings closer to zero, diffuse pollution dilution). A narrow standard
344 deviation implies that the weighting of that land cover is identifiable; a high mean weighting (e.g.
345 improved grassland in Figure 1c) implies that it is an important source of risk relative to other land
346 covers; a low weighting (e.g. rough grass or horticulture in Figure 1c) implies an important source of
347 dilution (i.e. it acts to dilute the nutrient concentrations in the catchment). High standard deviations (e.g.
348 ~ 0.3 for bog, moorland, non-rotational horticulture) indicate that we cannot identify the risk weighting for
349 that land cover either because it is uninfluential or because its influence is not identifiable due to
350 equifinality. Finally, we use the mean and standard deviation of the optimum risk weightings in a t-test to
351 identify the confidence with which we can reject the null hypothesis that the mean weightings are a result
352 of random noise. Where the risk weightings are important and identifiable the null hypothesis will be

353 rejected. Where they are either not important (mean risk close to 0.5) or not identifiable (standard
354 deviation close to 0.3) the null hypothesis will be accepted.

355 Note that: (1) areal effects (i.e. large area, low magnitude) are implicitly corrected for as the estimate of
356 risk is calculated with an upslope contributing precipitation weighting; and (2) differential connectivity
357 effects are corrected for through the delivery index. This latter point is important as the likelihood of
358 delivery will interact with the spatial distribution of a given land cover to determine the propensity with
359 which a location can both generate and deliver risk. Here, we are finding the land cover weighting
360 required for generation risk taking into account that different locations within the landscape have different
361 likelihoods of delivery.

362 <Figure 1 near here >

363 **2.3. Case study catchments**

364 The approach has been applied to eleven catchments across England and Wales (Figure 2a) that are
365 relatively data rich, either as a result of additional EA monitoring as part of the Catchment Sensitive
366 Farming programme (<http://bit.ly/EA-CSF>) or through ongoing academic research. Land cover and land
367 management (including livestock) data provide important indicators as to the potential source of
368 pollutants in a catchment. In particular, the relative percentage of agriculture versus urban may be
369 important with respect to the pathways and forms of delivery of contaminants from land to water. For
370 each of the eleven catchments, the relative balance between agriculture (arable and improved
371 grassland) and urban land covers is shown in Figure 2b. Rough grassland, woodland, moorland and bog
372 are grouped together as other in this graph. For agricultural land covers and diffuse pollution risk, the
373 ratio of improved grassland (pasture) to arable may be particularly important in characterising different
374 forms of diffuse pollution risk. We use a pasture-arable index (PAI) to reveal the difference (% area)
375 normalised to the total agricultural area: $PAI = (A - P) / (A + P)$; where: P is the percentage of the
376 catchment that is pasture; and A is the percentage of the catchment that is arable. Index values can
377 range from -1 (all pasture) to 1 (all arable). This index is plotted relative to the hydrological regime in
378 Figure 2c. The hydrological regime defines the connectivity between pollutant and river and is influenced
379 by the topographic gradients within a catchment and the properties of its soil and rock and can be
380 broadly evaluated in terms of the mean baseflow index. SCIMAP's hydrological treatment is most suited

381 to a surface and shallow subsurface flow regime, where residence times are short and flows are
382 predominantly lateral rather than vertical (i.e. a low base flow index; BFI).

383 <Figure 2 near here>

384 Catchments are distributed across England and Wales and range from: surface water to groundwater
385 dominated (captured through the catchment average BFI); pasture to arable dominated (captured
386 through the PAI); and predominantly upland to predominantly lowland. Upland catchments have higher
387 mean elevation, with more variability in elevation and (due to orographic rainfall enhancement) tend to
388 have higher catchment mean annual precipitation (MAP) and more variability in annual precipitation over
389 the catchment. To generalise the findings from these catchments we have compared the means and
390 standard deviations of the risk weightings for each land cover for N and P with a set of independent
391 variables chosen to describe the catchments' characteristics. We use: the Ordnance Survey coordinates
392 of the catchment centre point to represent their relative location; catchment area to define their size;
393 mean and standard deviation of elevation to describe their topography; mean and standard deviation of
394 mean annual precipitation to capture their rainfall conditions; mean base flow index to quantify the
395 relative dominance of ground water or surface water; the pasture arable index to capture the relative
396 dominance of pasture or arable land use; and the percentage cover of each land cover to establish the
397 influence of percentage cover on mean and standard deviation of risk weighting. We regressed these
398 catchment characteristics against means and standard deviations of risk weightings for each catchment
399 recording the best fit from linear, power, exponential and logarithmic least squares analysis.

400

401 **3. Results**

402 A detailed analysis of the results is given below for one of the catchments – the Hampshire Avon –
403 followed by more general analysis of the data across all eleven catchments. The detailed analysis serves
404 to demonstrate the methodology and to illustrate how the inferred land cover weightings can be used to
405 interpret diffuse pollution sources. The general analysis seeks to make substantive conclusions
406 regarding diffuse pollution processes across the 11 catchments considered.

407 **3.1. Example catchment – the Hampshire Avon**

408 The inverse approach provides information on the influence of land cover on in-stream nutrient
409 concentrations in the form of: (1) scatter plots (Figure 3a) and pdfs (Figure 3b) of the relationship
410 between model performance and risk weighting assigned to each land cover; (2) optimisation plots
411 (Figure 3c) showing the mean and standard deviation of the weightings for model runs which performed
412 better than a given threshold; (3) optimised mean weightings and their standard deviations from the best
413 0.5% of model runs (Table 2); and (4) t-test results to identify the confidence with which we can reject
414 the null hypothesis that the mean weightings are a result of random noise (Table 2). These pieces of
415 evidence then need to be interpreted to establish the contribution of each land cover to diffuse pollution
416 risk. In the following section we will: interpret these four outputs for woodland as an example; then show
417 how the outputs can be combined for all the Avon land covers; and finally interpret these to draw some
418 general conclusions about land cover types and diffuse pollution in the Avon.

419 <Figure 3 near here>

420 The dotted plots and pdfs (Figure 3a and b) show a strong negative relationship between model
421 performance and the risk weighting assigned to woodland areas (Table 2). The optimisation plots (Figure
422 3c) show a consistent decline in both the mean weighting and its standard deviation as the model runs
423 are refined to include only the best performances. For the optimum model performances: (1) mean
424 weightings are very low suggesting that woodland should be assigned a low risk to achieve the best
425 results; and (2) the standard deviation of the weightings is also very low suggesting that this weighting is
426 identifiable and can be assigned with a higher degree of certainty. Table 2 shows that woodland
427 weightings for the Avon are significantly different from the expected random weighting, at 99.9%
428 confidence for both P and N. These outputs from the inverse approach are summarised in Table 2 and
429 the outputs support one another to show that woodland is clearly identifiable as a low risk land cover and
430 is an important source of dilution for both P and N.

431

432 <Table 2 near here>

433 Table 2 shows that the different outputs from the inverse approach are often consistent in their indication
434 of a land cover's risk and the identifiability of that risk for a particular nutrient (e.g. rough grassland,

135 moorland, urban, cereals, horticulture) although they may differ between nutrients. In some cases there
136 are differences between the outputs for a single nutrient, such as improved grassland for P, where the
137 dotted plot and pdf indicate that it exerts some identifiable influence on model performance but the
138 significance test shows that its optimum risk weighting is not significantly different from the null case.
139 These cases highlight a need for careful examination of the outputs together. Often these conflicting
140 results suggest that the risk associated with a land cover is not identifiable but in some cases (e.g.
141 improved grass for P) they can highlight important information not captured in one or more of the
142 outputs.

143 Other land covers have no identifiable influence in all the outputs (dotted plots, pdfs, optimisation plots
144 and optimised values). Bog and non-rotational horticulture do not show identifiable patterns, for P or N
145 (Figure 3a and b), they have mean values close to 0.5 (Table 2) and standard deviations ~ 0.3 , the
146 expected values for a random sample from a uniform distribution. This may be because they have little
147 or no coverage in the Avon, highlighting an important property of our approach: it cannot make
148 predictions on the consequences of introducing new land cover types into the catchment. This is a
149 function of the inverse approach, which uses the land cover's influence on observations to define its risk
150 rather than defining it *a priori* (as in the forward approach).

151 Other land covers such as improved grassland cover a large proportion of the catchment but still display
152 considerable scatter in their dotted plots. This may reflect: (1) equifinality due to covariance in its coverage
153 with other land covers across the sub-catchments; (2) within class variability in the available nutrients; or
154 (3) unrepresented processes that disrupt the signal from this land cover.

155 In general, the results for the Avon suggest that woodland, rough grass and moorland are low risk land
156 covers for both P and N (Table 2). These land covers might be considered as sources of water with low
157 P and N concentrations that dilute rather than generate diffuse pollution. Woodland in particular is
158 consistently important as a 'diluting' land cover in the Avon. The differences in the strengths of
159 relationships between rough grass and moorland (Table 2) suggest that rough grass can be more
160 confidently identified as a source of dilution for P while moorland is more identifiable for N. It is important
161 to stress that the risk weightings that we have identified for land covers in the Avon are relative (rather
162 than absolute). As such, no matter how low the instream concentrations in a catchment, there will always
163 be some land covers contributing more nutrients and others contributing less (acting to dilute).

464 Land covers identified as high risk by the inverse approach appear to have differing signals according to
465 the nutrient being considered. Urban land cover appears an important source for P but not for N in the
466 Avon (Table 2, Figure 3), potentially linked to point source P inputs at sewage treatment works. Likewise,
467 horticulture appears to be an important source for P but is less important for N (Table 2). This may be
468 associated with excess nutrient applications to horticultural crops. Unpublished data using the
469 Phosphorus Indicators Tool (Heathwaite *et al.* 2003a) identified horticultural land cover as a high source
470 of P with a high delivery potential. Haygarth (2004) suggests that glass house and nursery stock pose a
471 high risk of nutrient loss through excess use of liquid fertiliser. Relative to the value of the crop the cost
472 of nutrient fertilizers is low. Cereals in the Avon have a low P risk (Table 2, Figure 3c) but very high N
473 risk and may be associated with locations that favour subsurface nutrient flux over surface runoff. The
474 spatial distribution of cereal crops in the Avon, which is predominantly chalk with a high Base Flow Index
475 (BFI, Table 8) tends to be focused on plateau areas some distance from receiving waters. Thus,
476 hydrological connection will be infrequent and delivery risk may be overestimated for nutrients which rely
477 on surface pathways for delivery, while those that can be effectively transported by groundwater flow will
478 remain connected.

479

480 **3.2. Extensive analysis of all 11 study catchments**

481 **3.2.1. Phosphorus**

482 For P, cereals and horticulture are an important source of risk (i.e. risk weighting significantly greater
483 than average 0.5) in only one catchment and three catchments respectively. Despite its limited coverage
484 non-rotational horticulture is an important source of risk in two other catchments (Table 3). This suggests
485 that arable land cover is sometimes a source of P in UK catchments. However it is neither the most
486 consistent nor the most dominant source. Urban land covers require a high risk weighting in nine out of
487 eleven catchments, with seven of these requiring a weighting greater than 0.77 (Table 3). Improved
488 grassland is important (i.e. has risk weightings that are significantly different from the null case) in six of
489 the eleven catchments but has an above average weighting in only three of these (Table 3). The risk
490 weightings for land covers associated with extensive land use practices (e.g. rough grass, moorland and
491 woodland) are clearly identifiable (they have low standard deviations) and are generally important

492 sources of dilution (they have low mean risks). Rough grass has significant weightings in ten of the
493 eleven catchments and needs to be given a low weighting (<0.23) in all of these (Table 3). Moorland and
494 woodland weightings are significant in fewer catchments (3 for each) but almost always require a low
495 weighting. Bogs cover only a very small proportion of any catchment and have no significant weightings.

496 < Table 3 near here >
497

498 **3.2.2. Nitrogen**

499 For N, one or more arable land covers are an important source of risk in eight out of eleven catchments.
500 Of the remaining three, urban land cover is important for two catchments and improved grassland for the
501 other. Cereals, horticulture and non-rotational horticulture appear to represent an important source of
502 risk in five, five and two catchments respectively (Table 4). Improved grassland appears to be a more
503 important land cover for N than for P, although its influence is still highly variable. It has significant
504 weightings in eight of the eleven catchments but has an above average weighting in only four of these
505 (Tables 3 and 4). For the extensive land uses (rough grass, moorland, woodland) the results for N are
506 broadly similar to P. Rough grass has a significant weighting in fewer catchments for N as compared
507 with P (eight out of eleven) but must be given a low weighting in all of these catchments. Woodland has
508 a significant weighting in seven catchments and is generally low risk (<0.19 for five catchments) but
509 occasionally a source of risk (>0.69 for two catchments). Moorland has more significant weightings in
510 more catchments for N than for P, and almost always requires a low weighting with seven catchments in
511 which its risk weighting must be set to <0.36 (although it has a high weighting for the Frome).

512 <Table 4 near here >
513

514 **3.2.3. Land cover areal extent effects**

515 Tables 3, 4 and 5 show that, notwithstanding the upslope contributing precipitation weighting, the land
516 covers that exert a significant influence on model performance are often those that cover the largest
517 proportion of the catchment. We explored this observation by considering the standard deviation (SD) of
518 the risk weightings from the best 0.5 % of model runs for each land cover for each nutrient. Lower
519 standard deviations imply that a particular land cover has a risk weighting that is clearly identifiable using

520 the inverse approach. Generally, as the area covered by a given land cover increases, so the standard
521 deviation becomes narrower (Figure 4). Non-rotational horticulture, which has generally low catchment
522 cover, has a range of standard deviation values, suggesting that its identifiability varies between
523 catchments, and is generally uninfluenced by the proportion of the catchment it covers (Figure 4a and c).
524 Urban land cover accounts for <10% of all catchments studied but often has a low standard deviation
525 (indicating that its risk weighting is often clearly identifiable) and appears to be independent of
526 percentage cover. Cereals and horticulture vary in percentage cover from 2% to 36% but the standard
527 deviations are negatively correlated with the percentage cover (**Error! Reference source not found.**),
528 suggesting that where these land covers have a high spatial coverage they tend to be clearly identifiable
529 (Figure 4a and c). Improved grassland often has a very large share of the catchment but there is no
530 negative relationship between percentage cover and standard deviation. Even high percentage covers
531 have high standard deviations. This suggests that the weighting associated with improved grassland is
532 often very difficult to identify even when it makes up a very large proportion of the catchment. As in the
533 specific case of the Avon, this may reflect: equifinality due to covariance in its coverage with other land
534 covers; within class variability in the available nutrients; or unrepresented processes that disrupt its
535 influence.

536

537 <Table 5 and Figure 4 near here>

538 **3.2.4. Catchment Characteristics**

539 We have tested the ability of a set of independent variables that represent catchment characteristics to
540 predict the variance in both the mean (representing importance as a source of risk or dilution) and the
541 standard deviation (representing identifiability) of the risk weightings assigned to each land cover.

542 Percentage cover is consistently the most effective predictor of the standard deviation of the weightings
543 (**Error! Reference source not found.**). For P, it is the only significant predictor for 3 land covers
544 (horticulture, non-rotational horticulture and woodland) and the dominant predictor (highest r^2) for one
545 other (cereals). For N, it is the only significant predictor for one land cover (urban) and the dominant
546 predictor for two others (rough grass and moorland). In every case identifiability improves as percentage
547 cover increases. The other catchment characteristics have a less consistent influence on identifiability,
548 either in terms of the number of land covers that they influence or the direction of their influence (i.e. to

549 improve or reduce identifiability). There are only two land covers for P (rough grass and moorland) and
550 two for N (cereals and woodland) where another variable is a better predictor of identifiability than
551 percentage cover (**Error! Reference source not found.**).

552 For P, moving north across the UK, risk weightings for rough grass become more identifiable (negative
553 trend between northing and standard deviation of risk weighting $r^2=0.53$). The weightings for moorland
554 become less identifiable as catchments become more pasture rather than arable dominated; they
555 become more identifiable in upland catchments (where elevation and average annual rainfall are both
556 higher and more variable). For both N and P, the risk weighting for cereals becomes less identifiable in
557 upland catchments and more identifiable with distance east and in pasture dominated catchments
558 (**Error! Reference source not found.**). For P these relationships are weak relative to the strong
559 influence of percentage cover. Whereas for N the influence of percentage cover is weaker.

560 Percentage cover exerts little influence on mean weightings (it is a significant predictor in only four land
561 covers, all for N, and dominant in only one); instead, mean weightings are more effectively predicted by
562 other catchment characteristics (

563 Table 6). For P, moving north across the UK, mean risk weightings for rough grass tend to decrease while
564 those for improved grassland increase (

565 Table 6). Upland catchments have higher weightings for rough grass, improved grassland, urban areas
566 and horticulture. This is reflected in strong correlations with mean elevation and its variability and with
567 catchment average annual rainfall and its variability. The relationships between catchment characteristics
568 and the risk weighting assigned to improved grassland are particularly strong. Improved grassland risk
569 weightings increase significantly with distance north ($r^2=0.52$;

570 Table 6) and with increased variability in rainfall and elevation ($r^2=0.57$) suggesting that in upland-

571 dominated northern catchments, improved grassland constitutes a more important source of risk than for

572 lowland catchments in the south. However, the dominant control on improved grassland risk weighting

573 for P appears to be catchment average BFI ($r^2=0.91$). This suggests that improved grassland represents

574 a lower risk land cover for P in ground water than in surface water dominated catchments. These

575 relationships are much stronger than the very limited control that percentage cover exerts on the

576 improved grassland risk weighting ($r^2=0.05$).

577 <
578 Table 6 and 7 near here>

579 There are more significant relationships between catchment characteristics and mean risk weightings for
580 N than for P (

581 Table 6) suggesting that the mean risk weightings for N are more sensitive to these characteristics. This

582 is perhaps unsurprising given the dominance of urban point sources for P.

583 For N, northern catchments have lower risk weightings for rough grass ($r^2=0.43$) and high weightings for
584 woodland ($r^2=0.42$) while eastern catchments have high weightings for rough grass ($r^2=0.43$) but lower
585 for cereals and horticulture (r^2 of 0.44 and 0.57 respectively in

586 Table 6). As catchments become increasingly dominated by upland areas the risk weightings for rough
587 grass fall while the weightings for cereals and horticulture increase (
588 Table 6). This is unlikely to be related to differences in the percentage cover of these land covers in
589 upland and lowland catchments since percentage cover is a relatively weak predictor of weighting for
590 these covers. As catchments become increasingly groundwater rather than surface water dominated, the
591 weightings for woodland and improved grassland reduce (r^2 of 0.52 and 0.41 respectively in
592 Table 6).

593 **3.2.5. Overall Model Performance**

594 Table 8 shows the correlation coefficients of the best model performances for P and N. In general, the
595 results are encouraging and do suggest that this approach can reconcile a significant amount of the spatial
596 variability in the statutory water quality data used here. The results also suggest that SCIMAP is
597 calibrated more effectively for N than P.

598 Figure 5 suggests that SCIMAP performs well for upland catchments (positive correlation with mean and
599 standard deviation of catchment elevation) that have higher and more variable annual rainfall; while it
500 performs less well for catchments that are groundwater dominated (negative correlation with base flow
501 index) and predominantly arable (negative correlation with pasture arable index). The model is more
502 sensitive to these controls for N than P, and the model performance for Nitrate appears to be particularly
503 strongly controlled by variability in annual rainfall across the catchment and average elevation. These
504 two variables are likely to be strongly related to one another through the control that orographic rainfall
505 enhancement exerts on the spatial variability in rainfall across UK catchments. Maximum correlation
506 coefficients for N are very low for lowland catchments with little rainfall variability but rise very rapidly so
507 that they are all >0.8 for catchments with mean elevation >100 m and standard deviation of annual
508 rainfall >100 mm/a. These controls may reflect the hydrological basis of the analysis of connectivity used
509 here. In particular, the model's assumptions are best suited to catchments where steeper topographic
510 and hydraulic gradients and impermeable bedrock encourage lateral surface or subsurface flow rather
511 than deep infiltration and ground water flow. The recharge of streams by groundwater sources may both
512 dilute but also re-introduce N and P in ways that are not represented in our analysis.

513 <Table 8 and

514 Figure 5 near here>

515

516 **4. Discussion**

517 The relative risk weighting assigned to each land cover is not consistent across the 11 catchments
518 investigated here, suggesting that the importance of a particular land cover in contributing to a given in-
519 stream water quality parameter is both geographically-variable (across the study catchments considered)
520 and nutrient dependent (e.g. Table 3). This was confirmed by comparison of inferred risk weightings
521 with catchment characteristics (

522 Table 6). It implies that it will be difficult to identify universal nutrient availability risks for particular land
523 covers that can be applied to all catchments as in the export coefficient modelling approach (e.g.
524 Johnes, 1996; Johnes *et al.*, 2007) and the phosphorus indicators tool (Heathwaite *et al.*, 2003a, 2005a).
525 Thus, a careful consideration of catchment characteristics will be needed *a priori* in defining risky land
526 covers. Inverse approaches have a role to play in identifying for a given catchment and parameter (e.g.
527 nutrient) those land covers that are most likely to be sources. Approaching the inverse problem for water
528 quality without both a risk generation and a risk connection treatment is likely to be difficult because
529 spatial variability in connectivity and dilution effects may impart significant spatial variability on the water
530 quality data in ways that make finding the land cover signal particularly difficult.

531 The level of variability between catchments is surprising since we might expect the risk associated with
532 each land cover to be similar (at least in relative terms). To some extent, the variability may reflect
533 differences in risk availability on these land covers resulting from different land management practices
534 between catchments. However, it is also likely to reflect the spatial structure of the catchment in terms of
535 the dominance of particular land cover types (Davies and Neal, 2007;

536 Figure 4). Further, at least some of the variability in risk weighting may be related to an implicit
537 parameterisation of hydrological processes that are not currently represented in SCIMAP. This is
538 illustrated in the detailed analysis for the Hampshire Avon and the differences general improvement in
539 model performance in surface water dominated catchments (

540 Figure 5). Our results illustrate the importance of inverse approaches in situations such as this, where
541 there are known and possible process inadequacies that can't be dealt with easily through model
542 reformulation. Such inadequacies will be manifest as reductions in the extent to which good results (here
543 correlations with the water quality data) can be found.

544 We can be more certain about the land covers that represent low risks (rough grass, moorland and
545 woodland). These land covers are important since they act to dilute nutrient fluxes from other sources in
546 the catchment. This is perhaps unsurprising since they are areas expected to have little or no nutrient
547 application (Jackson, 2000). However, it is encouraging for the model that these land cover types are
548 consistently identified as low risk without any kind of *a priori* tuning. In fact the model highlights an
549 important point: that land uses like rough grazing, moorland and woodland have an important
550 contribution to make to the overall spatial signal of instream nutrient concentrations whilst they are
551 maintained in a low input state. If their status changes and their capacity to dilute is affected this may
552 have important consequences for water quality downstream.

553 In general terms, urban land covers tend to need high weightings for in-stream P concentrations in many
554 of the catchments. This is consistent with recent UK studies linking P concentrations to the percentage
555 urban cover (Rothwell *et al.*, 2010a), population density (Davies and Neal, 2004, 2007) and number of
556 known point sources (Rothwell *et al.*, 2010b) in catchments. It suggests the continued importance of
557 point source pollution for in-stream P concentrations, particularly from sewage treatment works (Jarvie *et al.*,
558 2006; Muscutt and Withers, 1996; Neal *et al.*, 2010b). A key advantage of the inverse approach used
559 here (taking account of possible bias of sample sites to urban areas) is that it is not necessary to
560 separate *a priori* a possible point signal from a non-point signal, so resolving the dilemma regarding the
561 relative significance of point and non-point sources. This significance is revealed through the analysis,
562 which identifies when non-urban sources are dominant.

563 For N, we found that arable areas were a more important source of risk. This is consistent with the
564 results of statistical analysis by Ferrier *et al.* (2001), who found nitrogen concentrations in Scottish rivers
565 to be highly correlated with the extent of arable land. Other UK studies also found that the extent of
566 arable land was a significant predictor for N but much less significant for P concentrations (Davies and
567 Neal, 2007; Rothwell *et al.*, 2010a, 2010b).

568 The optimum risk weightings do not identify improved grassland as a dominant driver for N or P, this is
569 surprising given the high levels of N and P application associated with this land cover (Johnes, 1996;
570 Johnes and Butterfield, 2002); and results from export coefficient modelling (Johnes *et al.*, 2007), which
571 highlight livestock waste as an important contributor to diffuse agricultural nutrient loading. However,
572 Davies and Neal (2007) also found no relation between grassland cover and P concentration suggesting
573 that the strong urban signal masks the contribution from improved grassland. The dotted plots for
574 individual catchments often show complex patterns for improved grassland. In some cases high risk
575 weightings producing reasonable model performances but low to medium risks were required for the
576 best model performances; and those low-medium risks then have the best and some of the worst model
577 performances. This may be in part a result of the true relative risk associated with improved grasslands,
578 which have intermediate nutrient application and availability. However, it may also reflect equifinality due
579 to covariance in its coverage with other land covers; the influence of unrepresented processes; or limits
580 to the available land cover data which are unable to distinguish between grasslands that are managed in
581 very different ways and as a result should be assigned different risk weightings (the model's data
582 requirements and the limits to current data are discussed in detail below).

583

584 An important distinction between our approach and others is our simple but explicit representation of the
585 probability that material will be delivered to the river network. There is a recognition in the literature: that
586 this probability of delivery is important in defining diffuse pollution risk (Beven *et al.*, 2005; Haygarth *et*
587 *al.*, 2005); that some parts of the catchment are more connected than others both in terms of the
588 frequency and duration of connection (Bracken and Croke, 2007; Jensco *et al.*, 2009; Lane *et al.*, 2009);
589 and that representing this connectivity is essential to effectively capturing delivery (Frey *et al.*, 2008;
590 Heathwaite *et al.*, 2005b; Neumann *et al.*, 2010). There is also a recognition that attempts to capture
591 connectivity and delivery resort to spatially explicit models that are data hungry and computationally
592 intensive (Neumann *et al.*, 2010; Radcliffe *et al.*, 2009); and that these models are too complex to
593 provide predictions at a fine enough resolution over areas large enough to be relevant for decision
594 making (Heathwaite, 2003; Neumann *et al.*, 2010). Our approach, using a simple static metric for
595 hydrological connectivity, which has been shown to capture both the frequency and duration of
596 connection (Lane *et al.*, 2009), enables us to run the model over large areas (e.g. ~2300 km² for the
597 River Eden catchment) at fine resolutions (<20m). Figure 3 shows that there is some uncertainty in the

598 inferred weightings that optimize our water quality measures. As it is easy to propagate these
599 uncertainties through the risk analysis, it provides the basis of balancing: the feasibility of the kind of
700 interventions that might reduce risk; their locations; their spatial extents; and the number of interventions;
701 given the uncertainties associated with particular land use effects. Any intervention will, equally, be
702 sensitive to changes in the spatial scale of impact: locations with a more certain land use weighting; that
703 are well-connected; and larger in extent are more likely to have effects that propagate through to larger
704 spatial scales. Changing small patches of land of a few 100 m² is unlikely to be detectable given these
705 uncertainties, but this approach still provides a means of delivering decision maker needs in relation to
706 the prioritization of sub-catchments and reaches (Heathwaite, 2003; Johnes *et al.*, 2007) and the spatial
707 extent over which prioritized reaches might impact downstream. We emphasise the need, however, to be
708 careful regarding spatial scale effects below. The model proceeds by time-integrated, rather than a
709 dynamic treatment of the system and a risk based rather than explicit nutrient balance approach. We feel
710 that these simplifications are appropriate in developing a tool for prioritization where time integrated
711 relative risk is the crucial factor; and given the available data. The difficulty with our approach is the
712 underpinning assumption of what element of the hydrological cycle drives water quality response, in this
713 case surface and shallow subsurface flows, and this is reflected in the poorer optimisation for
714 catchments with higher BFI and hence groundwater impacts.

715

716 Our model requires three sets of spatial information. Firstly, it requires information on the connectivity of
717 each location in the catchment to the river network. This is derived from fine resolution topographic data
718 under a set of assumptions and is used to define the delivery index. Given the availability of fine
719 resolution topographic data it is likely to be the assumptions (e.g. exponential decline in hydraulic
720 conductivity with depth, surface parallel water table; Lane *et al.*, 2006) rather than the data that limit this
721 component.

722

723 Secondly, the model requires a data set that identifies units of land that we expect to be similar in terms
724 of their nutrient availability (these are not limited to the land cover classes used here). The more
725 internally consistent these units are (i.e. the more between class rather than within class variability) the
726 more effective an inverse approach will be at identifying the risks associated with them. Therefore, the

727 suitability of our land cover based classes will be defined by: 1) the strength of the association between
728 land cover, land use and management; and 2) the spatial resolution at which the land cover can be
729 resolved, this will be particularly important in heterogeneous landscapes where there is a patchwork of
730 different land covers with different availabilities. This highlights an issue for diffuse pollution modelling if
731 the data on nutrient availability is limited both in spatial resolution and level of detail. In our case, satellite
732 derived land cover data are the best available data for the UK but are unable to distinguish between
733 grassland areas with very similar spectral signatures but very different management practices (e.g.
734 silage vs. permanent grazing). Some land cover classes (e.g. horticulture and cereals) are spectrally
735 very different but may reflect differences for that year rather than in the long term where both sets of
736 fields may be managed in the same way (e.g. crop rotation); the land use in these areas and as a result
737 the long term nutrient availability may be similar or even the same. In other settings, with better land
738 cover measurement systems, this may be less of an issue.

739

740 Finally, in-stream observations drive the risks assigned to these availability units (land covers), the
741 choice of observation will define the risks that are assigned. For example, different risk weightings
742 assigned to N and P in this study. These data need to reflect the interest for the catchment (e.g. N or P
743 in this study); they need to be time-integrated (in our case using the mean of the observations) but
744 representative (this can be particularly difficult for nutrients mobilized in storm events). The observations
745 need to be spatially rich and the inverse approach hinges on having observations sites that contain a mix
746 of land cover types and that mix being different from one observation point to the next. Large numbers of
747 observation points (e.g. >100 for the Eden catchment) will enable both a good mix of upstream land
748 covers and redundancy between points, ensuring that no single observation is defining the identified risk
749 weightings. Importantly though, this method does not require that the observation points are independent
750 of one another and as a result nested catchments and sub-catchments can all provide useful data for the
751 inverse approach.

752 In using this approach, we emphasise that there are three critical elements of the approach that may be
753 problematic. First, as we explained in the methodology, the observation that there is no systematic
754 relationship (e.g. in a 'dotty plot') between an Objective Function describing model performance and the
755 values of a land cover weighting has four different interpretations. First, the land cover does not exert an

756 influence on the model's performance and as such is not important either as a source of risk or dilution.
757 Second, the land cover does exert an influence on model performance but it is not identifiable as a result
758 of equifinality due to covariance in the coverage of land cover classes. Third, the data are inadequate to
759 resolve the influence of the land cover class (e.g. where nutrient availability is highly variable within a
760 class). Fourth, the model may not represent processes that are important in explaining the variability in
761 observed nutrient concentrations. In the second case, the available water quality data are unable to
762 resolve the influence of this land cover. If the analysis was undertaken over a smaller spatial scale, with
763 a very high density of monitoring sites, then this parameter might be shown to be important. This
764 analysis is, in effect, a relative one in that its findings apply to the spatial extent over which the water
765 quality data are available. Care must be shown in considering spatial units very much smaller or very
766 much larger than suggested by these data. However, we emphasise that when a systematic relationship
767 is found then this provides very important information at the scale of analysis over what is contributing to
768 the observed spatial variation in a water quality parameter. The second critical element of the approach
769 is related to the spatially-distributed water quality data themselves. Such datasets are rare and even
770 where available may not have sufficient temporal resolution to be representative of the actual water
771 quality signal at a point in a catchment. It is necessary to consider: (1) the representativeness of the
772 spatial distribution of sites; and (2) the representativeness of the temporal variability in water quality;
773 through a careful analysis of those data; before deciding to use them in the manner we demonstrate in
774 this manuscript. Third, some of the variability in the risk weightings between catchments may be related
775 to an implicit parameterisation of unrepresented hydrological processes (e.g. groundwater flow) arising
776 from incorrect assumptions in SCIMAP. Such assumptions are likely to be manifest in lower levels of
777 optimal agreement between predictions and observations and this level of agreement, in a Bayesian
778 approach, may be a useful wider indicator of the extent to which the assumptions being made in the
779 model are acceptable. Such an evaluation needs to be catchment-by-catchment, and checked against
780 other contextual data such as BFIs.

781 **5. Conclusion**

782 The inverse approach developed in this paper allows us to draw four broad conclusions. First, the
783 relative risk weightings assigned to each land cover are not consistent across all catchments, suggesting
784 that the importance of a particular land cover in contributing to river water quality is variable between

785 catchments. Second, some of this variability is due to catchment properties suggesting that diffuse
786 pollution policy needs to be carefully tuned on a catchment-by-catchment basis to reflect both the land
787 cover mix and catchment characteristics. Third, trends differ between the two nutrients, P and N,
788 considered here. For P, urban land covers are often high risk; rough grass and moorland are generally
789 low risk; improved grasslands are intermediate risk and arable land covers do not always require a high
790 risk weighting, although this may be partly because the measured water quality data are unable to
791 resolve arable land cover effects due to equifinality resulting from covariance in the coverage of arable
792 land covers. Point source pollution reflected in the weightings given to urban land covers appears to
793 exert a dominant control on in-stream P concentrations in many, but not all, catchments. For N, urban
794 land covers are less dominant and often low risk; rough grass and moorland remain low risk; and arable
795 land covers are generally important N sources in many catchments. This highlights the ability of our
796 analysis to identify when non-urban sources are dominant, resolving the dilemma regarding the relative
797 significance of point and non-point sources and negating the need for their *a priori* separation. Finally,
798 differences in the dominant pollution source depending on the pollutant raise intriguing questions about
799 whether they result from differences in nutrient availability or in delivery. Improved model performance
300 for N relative to P suggests that this is at least partly related to delivery and may reflect differences
301 between nutrients in: hydrologic flow paths; the extent to which they are conservative during transport;
302 and / or the ease with which they can be measured.

303 One final theme emerges from this paper: the kinds of generalisation that might be possible in relation to
304 possible diffuse pollution causes. Ideally, we would have shown that it is possible to isolate a subset of
305 predictors that can be used to profile diffuse pollution risks in any one catchment. Such a generalisation
306 would then allow the refinement of diffuse pollution policy. Work with further predictors might lead to
307 such a generalisation but such work may also be misplaced as it assumes that all the possible
308 candidates for a more complex generalisation are both known and quantifiable. The generalizable
309 element of this paper is not the relative importance of land covers, but rather a methodology that
310 combines a relatively simple model with spatially-distributed extant measurements, to infer the
311 parameters that matter. The simplicity of the model (and the associated Monte Carlo method) means
312 that the analysis is not computationally demanding, can be fully automated, and yields information on the
313 uncertainty of model findings simultaneously with model predictions. As such, it may be a preferable

314 approach than using a more complex model where the data and computational demands of a more
315 complex model cannot be readily met.

316 **Acknowledgements**

317 This project was funded by a NERC grant NE/C508850/1 awarded to S.N.L. and A.L.H. with additional
318 support from Defra, the Environment Agency and the Association of Rivers Trusts. The NERC Earth
319 Observation Data Centre provided free access to the IfSAR data. The contributions to this work from a
320 number of Environment Agency staff, but notably Chris Burgess, Linda Pope and Rob Willows, and also
321 from Chris Buckley (Durham University) and Trevor Page (Lancaster University) are gratefully
322 acknowledged. The views expressed in the manuscript are those of the authors and not the funding
323 bodies.

324

325 **References**

326 Beven K. Changing ideas in hydrology - the case of physically-based models. *J Hydrol* 1989; 105: 157-
327 172.

328 Beven K, Binley A. The future of distributed models: model calibration and uncertainty prediction. *Hydrol*
329 *Process* 1992; 6: 279-298.

330 Beven K. Prophecy, reality and uncertainty in distributed hydrological modelling. *Adv Water Resour*
331 1993; 16: 41-51.

332 Beven K, Heathwaite L, Haygarth P, Walling D, Brazier R, Withers P. On the concept of delivery of
333 sediment and nutrients to stream channels. *Hydrol Process* 2005; 19: 551-556.

334 Bracken LJ, Croke J. The concept of hydrological connectivity and its contribution to understanding
335 runoff-dominated geomorphic systems. *Hydrol Process* 2007; 21: 1749-1763.

336 Burt TP, Howden NJK, Worrall F, Whelan MJ, Bierozza M. Nitrate in United Kingdom rivers: policy and its
337 outcomes since 1970. *Environ Sci Technol* 2011; 45: 175-181.

338 CEH. Land Cover Map of Great Britain <http://www.ceh.ac.uk/data/lcm/>. Centre for Ecology Hydrology,
339 2000.

340 Collins AL, McGonigle DF. Monitoring and modelling diffuse pollution from agriculture for policy support:
341 UK and European experience. *Environ Sci Policy* 2008; 11: 97-101.

342 Davies H, Neal C. GIS-based methodologies for assessing nitrate, nitrite and ammonium distributions
343 across a major UK basin, the Humber. *Hydrol Earth Syst Sci* 2004; 8: 823-833.

344 Davies H, Neal C. Estimating nutrient concentrations from catchment characteristics across the UK.
345 *Hydrol Earth Syst Sci* 2007; 11: 550-558.

346 Doyle MW. Incorporating hydrologic variability into nutrient spiraling. *J Geophys Res* 2005; 110: G01003.

347 Easton ZM, Fuka DR, Walter MT, Cowan DM, Schneiderman EM, Steenhuis TS. Re-conceptualizing the
348 soil and water assessment tool (SWAT) model to predict runoff from variable source areas. *J Hydrol*
349 2008; 348: 279-291.

350 Edwards AC, Withers PJA. Transport and delivery of suspended solids, nitrogen and phosphorus from
351 various sources to freshwaters in the UK. *J Hydrol* 2008; 350: 144-153.

352 Ekholm P, Turtola E, Grönroos J, Seuri P, Ylivainio K. Phosphorus loss from different farming systems
353 estimated from soil surface phosphorus balance. *Agr Ecosyst Environ* 2005; 110: 266-278.

354 Ferrier RC, Edwards AC, Hirst D, Littlewood IG, Watts CD, Morris R. Water quality of Scottish rivers:
355 spatial and temporal trends. *Sci Total Environ* 2001; 265: 327-342.

356 Foresight_Landuse_Futures_Report. Final Project Report. The Government Office for Science, London.
357 2010,

358 Frey MP, Schneider MK, Dietzel A, Reichert P, Stamm C. Predicting critical source areas for diffuse
359 herbicide losses to surface waters: Role of connectivity and boundary conditions. *J Hydrol* 2009; 365:
360 23-36.

361 Fuller RM, Smith GM, Sanderson JM, Hill RA, Thomson AG. The UK land cover map 2000: construction
362 of a parcel-based vector map from satellite images. *Cartogr J* 2002; 39: 15-25.

363 Haygarth PM. Reviewing the potential for reductions of nitrogen and phosphorus inputs in current farm
364 systems. DEFRA, London, 2004.

365 Haygarth PM, Condron LM, Heathwaite AL, Turner BL, Harris GP. The phosphorus transfer continuum:
366 linking source to impact with an interdisciplinary and multi-scaled approach. *Sci Total Environ* 2005; 344:
367 5-14.

368 Heathwaite AL, Sharpley AN, Gburek WJ. A conceptual approach for integrating phosphorus and
369 nitrogen management at catchment scales. *J Environ Qual* 2000; 29: 158–166.

370 Heathwaite AL. Making process-based knowledge useable at the operational level: a framework for
371 modelling diffuse pollution from agricultural land. *Environ Modell Softw* 2003; 18: 753-760.

372 Heathwaite AL, Fraser AI, Johnes PJ, Hutchins M, Lord E, Butterfield D. The phosphorus indicators tool:
373 a simple model of diffuse P loss from agricultural land to water. *Soil Use Manage* 2003a; 19: 1-11.

374 Heathwaite AL, Sharpley AN, Beckmann M, Rekolainen S. Assessing the risk of agricultural nonpoint
375 source phosphorus pollution. In: Sims JT, Sharpley AN, editors. *Phosphorus: Agriculture and the*
376 *Environment*. ASA/CSSA/SSSA Monograph, 2003b.

377 Heathwaite AL, Dils RM, Liu S, Carvalho L, Brazier RE, Pope L, Hughes M, Phillips G, May L. A tiered
378 risk-based approach for predicting diffuse and point source phosphorus losses in agricultural areas. *Sci*
379 *Total Environ* 2005a; 344: 225-239.

380 Heathwaite AL, Quinn PF, Hewett CJM. Modelling and managing critical source areas of diffuse pollution
381 from agricultural land using flow connectivity simulation. *J Hydrol* 2005b; 304: 446-461.

382 Heathwaite AL. Multiple stressors on water availability at global to catchment scales: understanding
383 human impact on nutrient cycles to protect water quality and water availability in the long term.
384 *Freshwater Biol* 2010; 55: 241-257.

385 Hewett CJM, Quinn PF, Heathwaite AL, Doyle A, Burke S, Whitehead PG, Lerner DN. A multi-scale
386 framework for strategic management of diffuse pollution. *Environ Modell Softw* 2009; 24: 74-85.

387 Hilton J, O'Hare M, Bowes MJ, Jones JI. How green is my river? A new paradigm of eutrophication in
388 rivers. *Sci Total Environ* 2006; 365: 66-83.

389 Howden NJK, Burt TP, Worrall F, Whelan MJ, Bierzoza M. Nitrate concentrations and fluxes in the River
390 Thames over 140 years (1868–2008): are increases irreversible? *Hydrol Process* 2010; 24: 2657-2662.

391 Jackson DL. Guidance on the interpretation of the biodiversity broad habitat classification (terrestrial and
392 freshwater types): definitions and the relationship with other habitat classifications. JNCC Report, 307,
393 2000.

394 Jarvie HP, Neal C, Withers PJA. Sewage-effluent phosphorus: a greater risk to river eutrophication than
395 agricultural phosphorus? *Sci Total Environ* 2006; 360: 246-253.

396 Jencso KG, McGlynn BL, Gooseff MN, Wondzell SM, Bencala KE, Marshall LA. Hydrologic connectivity
397 between landscapes and streams: Transferring reach- and plot-scale understanding to the catchment
398 scale. *Water Resour Res* 2009; 45: W04428.

399 Johnes PJ. Evaluation and management of the impact of land use change on the nitrogen and
400 phosphorus load delivered to surface waters: the export coefficient modelling approach. *J Hydrol* 1996;
401 183: 323-349.

402 Johnes PJ, Heathwaite AL. Modelling the impact of land use change on water quality in agricultural
403 catchments. *Hydrol Process* 1997; 11: 269-286.

404 Johnes PJ, Butterfield D. Landscape, regional and global estimates of nitrogen flux from land to sea:
405 Errors and uncertainties. *Biogeochemistry* 2002; 57-58: 429-476.

406 Johnes PJ. Uncertainties in annual riverine phosphorus load estimation: Impact of load estimation
407 methodology, sampling frequency, baseflow index and catchment population density. *J Hydrol* 2007;
408 332: 241-258.

409 Johnes PJ, Foy R, Butterfield D, Haygarth PM. Land use scenarios for England and Wales: evaluation of
410 management options to support 'good ecological status' in surface freshwaters. *Soil Use Manage* 2007;
411 23: 176-194.

412 Jordan C, Mihalyfalvy E, Garrett MK, Smith RV. Modelling of nitrate leaching on a regional scale using a
413 GIS. *J Environ Manage* 1994; 42: 279-298.

414 Khadam IM, Kaluarachchi JJ. Water quality modeling under hydrologic variability and parameter
415 uncertainty using erosion-scaled export coefficients. *J Hydrol* 2006; 330: 354-367.

416 Kirchner JW, Feng X, Neal C, Robson AJ. The fine structure of water-quality dynamics: the (high-
417 frequency) wave of the future. *Hydrol Process* 2004; 18: 1353-1359.

018 Kirchner JW. Getting the right answers for the right reasons: linking measurements, analyses, and
019 models to advance the science of hydrology. *Water Resour Res* 2006; 42: W03S04.

020 Lane SN, Brookes CJ, Heathwaite AL, Reaney S. Surveillant science: challenges for the management of
021 rural environments emerging from the new generation diffuse pollution models. *J Agr Econ* 2006; 57:
022 239-257.

023 Lane SN. What makes a fish (hydrologically) happy? A case for inverse modelling. *Hydrol Process* 2008;
024 22: 4493-4495.

025 Lane SN, Reaney SM, Heathwaite AL. Representation of landscape hydrological connectivity using a
026 topographically driven surface flow index. *Water Resour Res* 2009; 45: W08423.

027 Lazar AN, Butterfield D, Futter MN, Rankinen K, Thouvenot-Korppoo M, Jarritt N, Lawrence DSL, Wade
028 AJ, Whitehead PG. An assessment of the fine sediment dynamics in an upland river system: INCA-Sed
029 modifications and implications for fisheries. *Sci Total Environ* 2010; 408: 2555-2566.

030 LWEC. Living With Environmental Change <http://www.lwec.org.uk/>, 2011.

031 Matthews R. The people and landscape model (PALM): towards full integration of human decision-
032 making and biophysical simulation models. *Ecol Model* 2006; 194: 329-343.

033 Mosegaard K, Tarantola A. Monte Carlo sampling of solutions to inverse problems. *J Geophys Res*
034 1995; 100: 12431-12447.

035 Mosegaard K, Tarantola A. Probabilistic approach to inverse problems. In: *International Handbook of*
036 *Earthquake & Engineering Seismology (Part A)*. Academic Press, 2002, pp. 237-265.

037 Munafò M, Cecchi G, Baiocco F, Mancini L. River pollution from non-point sources: a new simplified
038 method of assessment. *J Environ Manage* 2005; 77: 93-98.

039 Muscutt AD, Withers PJA. The phosphorus content of rivers in England and Wales. *Water Res* 1996; 30:
040 1258-1268.

041 Neal C, Jarvie HP, Williams R, Love A, Neal M, Wickham H, Harman S, Armstrong L. Declines in
042 phosphorus concentration in the upper River Thames (UK): Links to sewage effluent cleanup and
043 extended end-member mixing analysis. *Sci Total Environ* 2010a; 408: 1315-1330.

344 Neal C, Jarvie HP, Withers PJA, Whitton BA, Neal M. The strategic significance of wastewater sources
345 to pollutant phosphorus levels in English rivers and to environmental management for rural, agricultural
346 and urban catchments. *Sci Total Environ* 2010b; 408: 1485-1500.

347 Neumann LN, Western AW, Argent RM. The sensitivity of simulated flow and water quality response to
348 spatial heterogeneity on a hillslope in the Tarrawarra catchment, Australia. *Hydrol Process* 2010; 24: 76-
349 86.

350 Oreskes N, Shrader-Frechette K, Belitz K. Verification, validation, and confirmation of numerical models
351 in the earth sciences. *Science* 1994; 263: 641-646.

352 Page T, Haygarth PM, Beven KJ, Joynes A, Butler T, Keeler C, Freer J, Owens PN, Wood GA. Spatial
353 variability of soil phosphorus in relation to the topographic index and critical source areas: sampling for
354 assessing risk to water quality. *J Environ Qual* 2005; 34: 2263-2277.

355 Perry MC, Hollis DM. The generation of monthly gridded datasets for a range of climatic variables over
356 the UK. *Int J Climatol* 2005; 25: 1041-1054.

357 Pionke HB, Gburek WJ, Sharpley AN. Critical source area controls on water quality in an agricultural
358 watershed located in the Chesapeake Basin. *Ecol Eng* 2000; 14: 325-335.

359 Priess JA, de Koning GHJ, Veldkamp A. Assessment of interactions between land use change and
360 carbon and nutrient fluxes in Ecuador. *Agr Ecosyst Environ* 2001; 85: 269-279.

361 Quinn P. Scale appropriate modelling: representing cause-and-effect relationships in nitrate pollution at
362 the catchment scale for the purpose of catchment scale planning. *J Hydrol* 2004; 291: 197-217.

363 Radcliffe DE, Freer J, Schoumans O. Diffuse phosphorus models in the United States and Europe: their
364 usages, scales, and uncertainties. *J Environ Qual* 2009; 38: 1956-1967.

365 Reaney SM, Lane SN, Heathwaite AL, Dugdale LJ. Risk-based modelling of diffuse land use impacts
366 from rural landscapes upon salmonid fry abundance. *Ecol Model* 2011; 222: 1016-1029.

367 Rothwell JJ, Dise NB, Taylor KG, Allott TEH, Scholefield P, Davies H, Neal C. Predicting river water
368 quality across north west England using catchment characteristics. *J Hydrol* 2010a; 395: 153-162.

369 Rothwell JJ, Dise NB, Taylor KG, Allott TEH, Scholefield P, Davies H, Neal C. A spatial and seasonal
370 assessment of river water chemistry across north west England. *Sci Total Environ* 2010b; 408: 841-855.

071 Sharpley AN, Kleinman PJA, Heathwaite AL, Gburek WJ, Weld JL, Folmar GJ. Integrating contributing
072 areas and indexing phosphorus loss from agricultural watersheds. *J Environ Qual* 2008; 37: 1488-1496.

073 Sharpley AN, Matlock M, Heathwaite AL, Simpson T. Managing agricultural catchments to sustain
074 production and water quality. In: Ferrier R, Jenkins A, editors. *Handbook of Catchment Management*.
075 Blackwell Press, Chichester, 2009, pp. 560.

076 Siber R, Stamm C, Reichert P. Modeling potential herbicide loss to surface waters on the Swiss plateau.
077 *J Environ Manage* 2009; 91: 290-302.

078 Vatn A, Bakken L, Bleken MA, Baadshaug OH, Fykse H, Haugen LE, Lundekvam H, Morken J, Romstad
079 E, Rørstad PK, Skjelvåg AO, Sogn T. A methodology for integrated economic and environmental
080 analysis of pollution from agriculture. *Agr Syst* 2006; 88: 270-293.

081 Vrugt JA, ter Braak CJF, Gupta HV, Robinson BA. Equifinality of formal (DREAM) and informal (GLUE)
082 Bayesian approaches in hydrologic modeling? *Stoch Env Res Risk A* 2009; 23: 1011–1026.

083 Wade AJ, Whitehead PG, Butterfield D. The integrated catchments model of phosphorus dynamics
084 (INCA-P), a new approach for multiple source assessment in heterogeneous river systems: model
085 structure and equations. *Hydrol Earth Syst Sci* 2002; 6: 583-606.

086 Walling DE, Webb BW. Estimating the discharge of contaminants to coastal waters by rivers: Some
087 cautionary comments. *Mar Pollut Bull* 1985; 16: 488-492.

088 Weld J, Sharpley AN. Phosphorus indices. In: Radcliffe DE, Cabrera ML, editors. *Modeling phosphorus*
089 *in the environment*. CRC Press, Boca Raton, FL, 2007, pp. 301–332.

090 Whitehead PG, Heathwaite AL, Flynn NJ, Wade AJ, Quinn PF. Evaluating the risk of non-point source
091 pollution from biosolids: integrated modelling of nutrient losses at field and catchment scales. *Hydrol*
092 *Earth Syst Sci* 2007; 11: 601-613.

093

094

095

Table 1: Centre for Ecology and Hydrology Land Cover Map for 2000 classes and their translation to SCIMAP classes. Land covers that were either absent from the catchments or expected to contribute zero risk are classed as other (modified from Jackson, 2000 and Fuller *et al.*, 2002).

Land cover	Description	SCIMAP Class
Broad-leaved woodland	1.1 deciduous, mixed, open birch, scrub	Woodland
Coniferous woodland	2.1 conifers, felled, new plantation	Woodland
Arable cereals	4.1 barley, maize, oats, wheat, cereal (spring), cereal (winter)	Cereals
Arable horticulture	4.2 arable bare ground, carrots, field beans, linseed, potatoes, peas, oilseed rape, sugar beet, mustard, non-cereal (spring)	Horticulture
Non rotational horticulture	4.3 orchard, arable grass (ley), setaside	Non Rotational Horticulture
Improved grassland	5.1 intensive, grass (hay/ silage cut), grazing marsh	Improved grassland
Set aside grass	5.2 grass set aside	Rough grass
Neutral grass	6.1 rough grass (unmanaged), grass (neutral / unimproved)	Rough grass
Calcareous grass	7.1 calcareous (managed), calcareous (rough)	Rough grass
Acid grass	8.1 acid, acid (rough), acid with <i>Juncus</i> , acid with <i>Nardus/Festuca/Molinia</i>	Rough grass
Bracken	9.1 Bracken	Rough grass
Dwarf shrub heath	10.1 dense ericaceous, gorse	Moorland
Open dwarf shrub heath	10.2 ericaceous, gorse	Moorland
Fen, marsh, swamp	11.1 swamp, fen/marsh, fen willow	Bog
Bog	12.1 bog: shrub, grass/shrub, undifferentiated (all on deep peat)	Bog
Water (inland)	13.1 water (inland)	Other
Montane habitats	15.1 Montane	Moorland
Inland Bare Ground	16.1 despoiled, semi-natural	Other
Suburban/rural developed	17.1 suburban/rural developed	Urban
Continuous Urban	17.2 urban residential/commercial, urban industrial	Urban
Supra-littoral rock	18.1 Rock	Other
Supra-littoral sediment	19.1 shingle, shingle (vegetated), dune, dune shrubs	Other
Littoral rock	20.1 rock, rock with algae	Other
Littoral sediment	21.1 mud, sand, sand/mud with algae	Other
Saltmarsh	21.2 saltmarsh, saltmarsh (grazed)	Other
Sea / Estuary	22.1 Sea	Other

Table 2: a summary of the influence of each land cover type on Orthophosphate (PO₄³⁻-P) and Nitrate (NO₃⁻-N) risk inferred from inverse modelling for the Hampshire Avon including: a description of the relationship between risk weighting and model performance from the dotted plots and pdfs; the mean and standard deviation of the optimum risk weightings; and whether these mean risks were significantly different from those expected from random sampling. Bog land cover is not listed since it is not present in the Avon.

Land cover type	Cover (%)	Orthophosphate				Nitrate			
		Correlation risk v model fit	Optimum mean/standard deviation	Signif	Summary of Influence on P risk	Correlation risk v model fit	Optimum mean/standard deviation	Signif	Summary of Influence on N risk
Improved grassland	29	weak (+)	0.61/0.23	no	medium risk	none	0.57/0.25	no	not influential
Rough grass	11	weak (-)	0.24/0.16	99%	low risk	v weak (-)	0.27/0.19	95%	low risk
Moorland	2	weak (-)	0.28/0.21	95%	low risk	strong (-)	0.09/0.09	99.9%	low risk
Urban	8	weak (+)	0.65/0.26	90%	high risk	none	0.44/0.29	no	not influential
Cereals	22	strong (-)	0.16/0.08	99.9%	low risk	v strong (+)	0.78/0.18	99%	v high risk
Horticulture	14	v strong (+)	0.83/0.13	99%	v high risk	weak (+)	0.69/0.19	95%	High risk
Non rotational Horticulture	1	none	0.45/0.30	no	not influential	none	0.53/0.29	no	not influential
Woodland	13	strong (-)	0.12/0.09	99.9%	v low risk	v strong (-)	0.05/0.04	99.9%	v low risk

Table 3: optimised land cover risk weightings from SCIMAP based on the GQA in-stream Orthophosphate (PO₄³⁻-P) measurements in 11 UK catchments. Mean risk weightings that are significantly different from those expected based on random sampling with >90% (bold), 95% (*), 99% (**), and 99.9% (***) confidence are in red where they are high and blue where they are low risks. Blank entries result where that land cover is absent from a catchment.

Land cover	Avon	Deben	Eden	Frome	Rother	Slapton	Till	Wensum	Wye	Wyre	Yealm
Improved grassland	0.61	0.40	0.38	0.06 ***	0.57	0.56	0.71 *	0.13 ***	0.65	0.75 **	0.22 **
Rough grass	0.24 **	0.09 ***	0.16 ***	0.23 **	0.42	0.31 *	0.07 ***	0.16 ***	0.34 *	0.13 ***	0.16 ***
Moorland	0.28 *	0.36	0.19 **	0.50		0.51	0.41		0.12 ***	0.52	0.37
Bog		0.48	0.62	0.50			0.59	0.46	0.55	0.45	0.48
Urban	0.65	0.13 ***	0.82 **	0.69 *	0.82 **	0.77 **	0.77 **	0.85 ***	0.78 **	0.30 *	0.87 ***
Cereals	0.16 ***	0.84 ***	0.65	0.34 *	0.09 ***	0.32 *	0.24 **	0.18 **	0.29 *	0.55	0.31 *
Horticulture	0.83 **	0.28 *	0.51	0.13 ***	0.15 ***	0.69 *	0.53	0.24 **	0.78 **	0.16 ***	0.40
Non Rotational Horticulture	0.45	0.31 *	0.65	0.68 *	0.44			0.53	0.53		
Woodland	0.12 ***	0.31 *	0.14 ***	0.71 *	0.11 ***	0.46	0.51	0.47	0.35	0.60	0.45

Table 4: optimised land cover risk weightings from SCIMAP based on the GQA in-stream Nitrate (NO₃⁻-N) measurements in 11 UK catchments. Mean risk weightings that are significantly different from those expected based on random sampling with >90% (bold), 95% (*), 99% (**), and 99.9% (***) confidence are in red where they are high and blue where they are low risks. Blank entries result where that land cover is absent from a catchment.

Land cover	Avon	Deben	Eden	Frome	Rother	Slapton	Till	Wensum	Wye	Wyre	Yealm
Improved grassland	0.57	0.66	0.56	0.02 ***	0.26 **	0.77 **	0.72 *	0.06 ***	0.42	0.71 *	0.37
Rough grass	0.27 *	0.21 **	0.12 ***	0.43	0.29 *	0.62	0.10 ***	0.52	0.13 ***	0.16 ***	0.14 ***
Moorland	0.09 ***	0.36	0.15 ***	0.65		0.44	0.09 ***		0.22 **	0.19 **	0.08 ***
Bog		0.66	0.53	0.52			0.49	0.54	0.64	0.49	0.54
Urban	0.44	0.83 **	0.40	0.56	0.87 ***	0.25 *	0.58	0.45	0.58	0.06 ***	0.85 ***
Cereals	0.78 **	0.63	0.73 *	0.56	0.11 ***	0.64	0.56	0.04 ***	0.69 *	0.52	0.56
Horticulture	0.69 *	0.14 ***	0.63	0.49	0.26 **	0.85 ***	0.87 **	0.77 **	0.80 **	0.64	0.41
Non Rotational Horticulture	0.53	0.42	0.72 *	0.80 **	0.52			0.43	0.61		
Woodland	0.05 ***	0.14 ***	0.10 ***	0.59	0.19 **	0.35	0.69 *	0.55	0.17 ***	0.71 *	0.44

Table 5: the percentage area covered by each of the SCIMAP land cover classes for each of the catchments under consideration.

Land cover	Avon	Deben	Eden	Frome	Rother	Slapton	Till	Wensum	Wye	Wyre	Yealm
Improved grassland	28.6	4.4	44.3	29.1	30.4	35.5	20.3	7.9	32.8	42.9	36.0
Rough grass	11.2	12.5	25.2	4.8	10.0	8.3	14.8	6.5	30.1	13.8	17.5
Moorland	1.6	0.8	7.6	4.9	0.0	0.1	5.1	0.0	4.8	6.0	5.7
Bog	0.0	0.6	2.8	0.3	0.0	0.0	0.8	0.1	0.2	1.9	0.5
Urban	8.1	7.2	2.6	7.5	5.3	7.1	1.3	6.9	3.9	10.8	7.5
Cereals	22.2	31.3	2.9	21.1	15.6	24.5	25.8	36.0	4.8	3.6	13.5
Horticulture	13.9	28.4	1.6	14.4	18.0	12.9	23.5	32.9	8.5	13.4	7.1
Non Rotational Horticulture	1.3	2.4	2.9	2.8	0.3	0.0	0.0	0.1	0.1	0.0	0.0
Woodland	12.8	8.3	8.8	12.5	19.1	6.9	7.5	9.2	14.2	4.7	10.9

Table 6: r^2 values for significant correlations (>95% confidence) between catchment characteristics and the mean risk weighting for each catchment for a given land cover. Red text indicates positive correlations blue text indicates negative correlations. Bold text indicates r^2 values significantly different from zero at 99.9% confidence.

Land cover	Northing	Easting	MAP	MAP sigma	Elevation	Elevation Sigma	BFI	% cover
Improved grassland	0.52 (P)			0.42 (P)		0.57 (P)	0.91 (P) 0.41 (N)	0.41 (N)
Rough grass	0.41 (P) 0.43 (N)	0.43 (N)		0.43 (N)	0.43 (N)	0.76 (N)		0.56 (N)
Urban					0.32 (P)			0.66 (N)
Cereals		0.44 (N)			0.33 (N)	0.31 (N)		
Horticulture		0.56 (N)	0.35 (N)	0.39 (N)	0.45 (P) 0.56 (N)			
Woodland	0.42 (N)						0.52 (N)	0.47 (N)

Table 7: r^2 values for significant correlations (>95% confidence) between catchment characteristics and the standard deviation of risk weighting for each catchment for a given land cover. Red text indicates positive correlations blue text indicates negative correlations. Bold text indicates r^2 values significantly different from zero at 99.9% confidence.

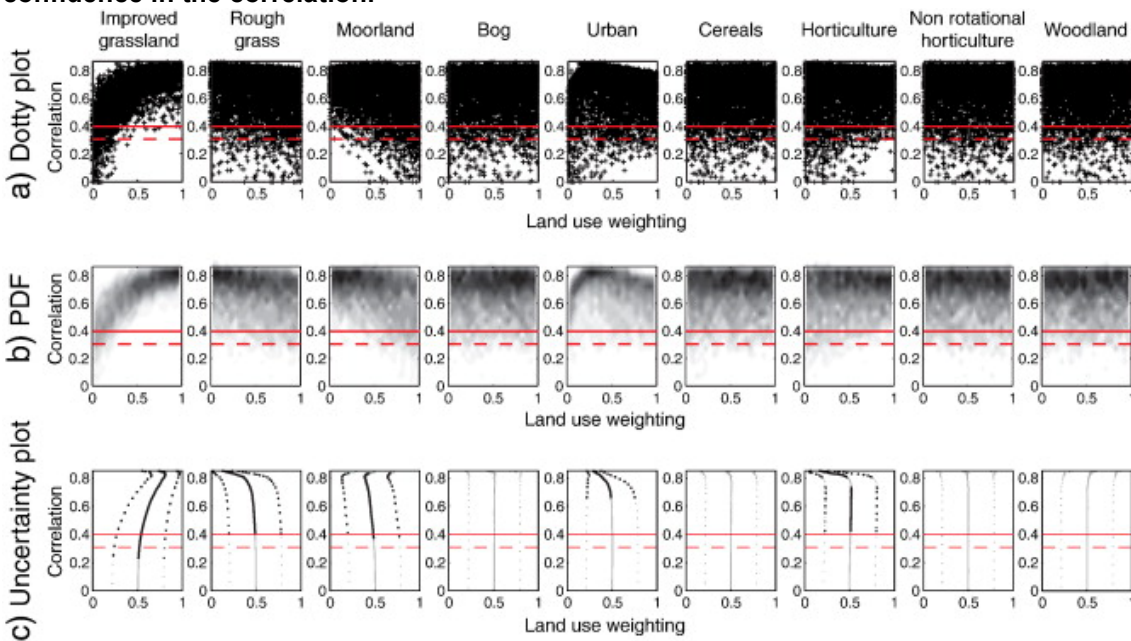
Land cover	Northing	Easting	Area	MAP	MAP sigma	Elevation	Elevation Sigma	PAI	% cover
Rough grass	0.53 (P)				0.42 (N)	0.46 (N)	0.51 (N)		0.88 (N)
Moorland				0.40 (P)	0.66 (P)	0.64 (P)	0.54 (P) 0.41 (N)	0.54 (P)	0.47 (P) 0.52 (N)
Urban									0.33 (N)
Cereals		0.50 (N)		0.42 (P) 0.38 (N)	0.39 (P) 0.36 (N)		0.34 (P) 0.57 (N)	0.46 (P) 0.42 (N)	0.77 (P) 0.39 (N)
Horticulture									0.44 (P)
Non rotational horticulture									0.35 (P)
Woodland			0.36 (N)						0.41 (P)

Table 8: correlation coefficients for the optimum SCIMAP model performance based on the GQA in-stream measurements of Orthophosphate ($\text{PO}_4^{3-}\text{-P}$), and Nitrate ($\text{NO}_3^-\text{-N}$) in 11 UK catchments with the values for independent variables used to represent catchment characteristics. The Ordnance Survey grid reference of the catchment centre point; mean and standard deviation of mean annual rainfall; mean and standard deviation of elevation; catchment area; the pasture arable index; and mean base flow index. Correlation coefficients are labelled where they are significant with 95% (*) and 99.9% (**) confidence.

Catchment	OS Grid Reference	Mean (σ) annual rainfall (mm/a)	Mean (σ) elevation (m)	Area (km^2)	Pasture -Arable Index	Base Flow Index	Optimum Correlation Coefficients	
							Orthophosphate	Nitrate
Avon	407200,136491	806 (47)	120 (47)	1716	0.13	0.87	0.71** (n=54)	0.89** (n=50)
Deben	629571,254581	582 (10)	29 (18)	745	0.87	0.58	0.68** (n=32)	0.57** (n=32)
Eden	355981,534572	1162 (328)	242 (153)	2274	-0.71	0.48	0.71** (n=80)	0.86** (n=80)
Frome	377582,92295	892 (50)	88 (62)	867	0.14	0.70	0.36* (n=48)	0.60** (n=40)
Rother	580450,126894	775 (52)	47 (42)	571	0.05	0.42	0.63** (n=41)	0.72** (n=38)
Slapton	277209,44517	1023 (69)	81 (46)	135	0.03	0.61	1.00** (n=6)	0.99** (n=6)
Till	393953,634235	725 (86)	137 (129)	1286	0.42	0.46	0.77** (n=25)	0.93** (n=25)
Wensum	599667,320954	661 (20)	49 (16)	699	0.79	0.64	0.78** (n=17)	0.28 (n=17)
Wye	321295,243964	1063 (288)	242 (140)	3049	-0.42	0.54	0.83** (n=108)	0.92** (n=107)
Wyre	347216,444615	1099 (173)	77 (112)	561	-0.43	0.44	0.87** (n=37)	0.92** (n=37)
Yealm	261514,55322	1300 (212)	144 (123)	215	-0.27	0.57	0.66* (n=16)	0.96** (n=16)

051 **Figures**

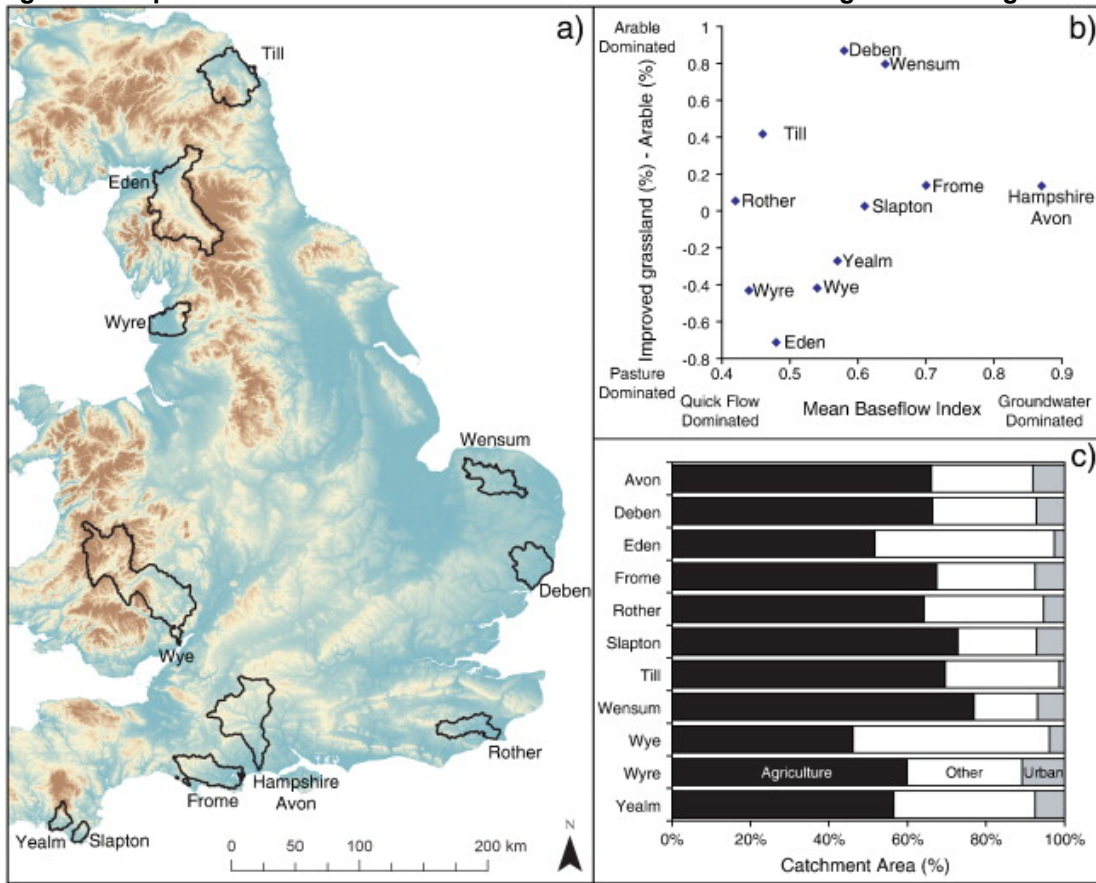
052 **Figure 1: Illustrative outputs from SCIMAP. Figure 1a shows the ‘dotty plots, the correlation achieved for**
053 **each simulation associated with the land cover risk weighting in that simulation. Figure 1b expresses the**
054 **dotty plots in Figure 1a as two dimensional probability density functions. Darker areas indicate a high**
055 **density of points within the ‘dotty plot’ and therefore a high probability that SCIMAP predictions with that**
056 **land cover risk weighting will fit the observations with that correlation coefficient (assuming random**
057 **sampling for all other land cover weightings). Figure 1c shows the mean and standard deviation of**
058 **weightings associated with correlations at or above the values shown on the y-axis; the lines are bold**
059 **where the risk weighting is significantly different from the null (no influence) case with 95 % confidence. In**
060 **each plot the red horizontal lines show correlation values required for 95 % (dashes), and 99 % (solid)**
061 **confidence in the correlation.**



062

063
 064
 065
 066
 067
 068
 069

Figure 2: Catchment properties for the eleven study catchments. Figure 2a shows the location of each catchment in the UK superimposed on a topographic map. Figure 2b shows the percentage area of each catchment that is managed for agriculture (arable and improved grassland) compared to that which is urban to provide some indication of the relative impact of diffuse relative to point source pollution. The rest of the land cover classes are grouped together as 'other'. Figure 2c shows the hydrologic and agricultural setting for each catchment by plotting base flow index as an indicator of hydrologic regime against the pasture-arable index as an indicator of the dominant agricultural regime within the catchment.

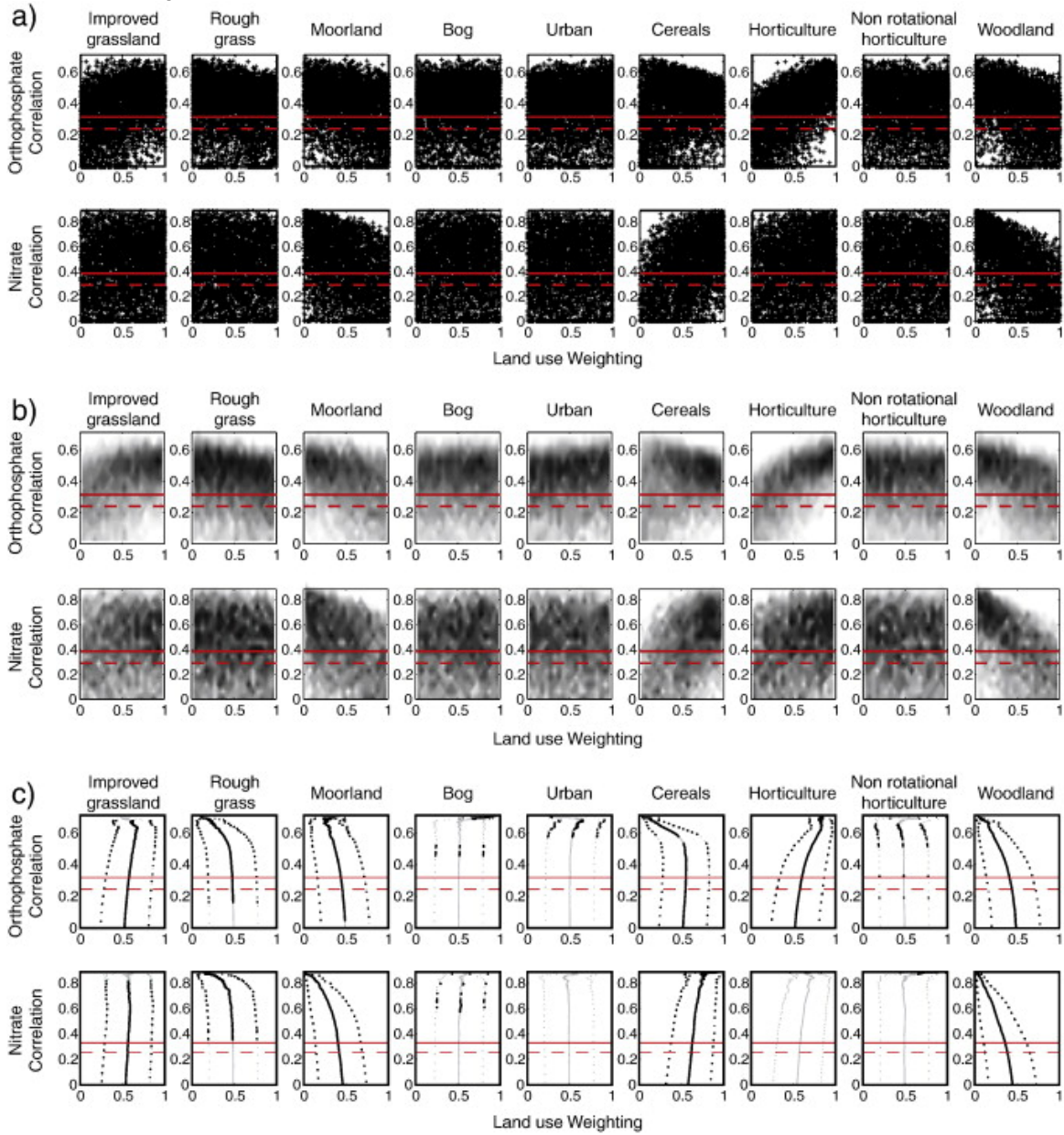


070

071

072
073
074
075
076
077
078

Figure 3: Model results for P and N in the (Hampshire) Avon. 3a shows the dotted plots, 3b the two-dimensional probability density functions, and 3c the risk weighting optimisation plots, showing the mean (solid line) and standard deviation (dashed line) of the weightings associated with correlations with GQA data greater than or equal to the associated correlation; the lines are bold where the risk weighting is significantly different from the null (no influence) case with 95 % confidence. Red horizontal lines show correlation values required for 95 % (dashes), and 99 % (solid) confidence in the correlation. In each section the top row shows results for P and the bottom row for N.

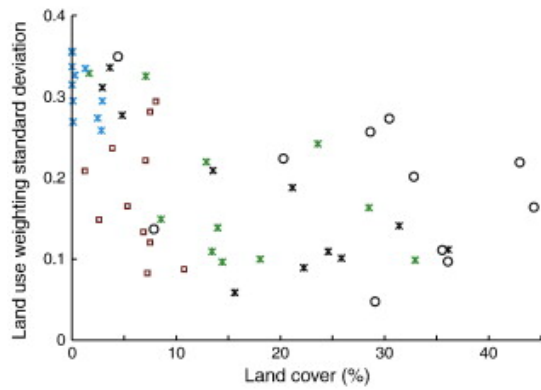


079
080

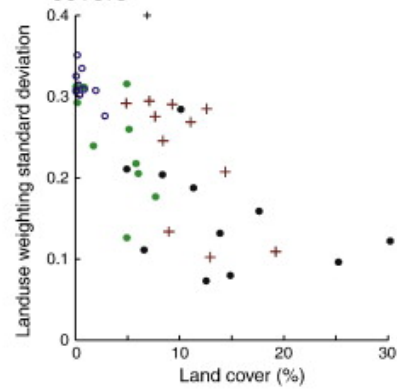
081
082
083
084
085

Figure 4: Scatter plots comparing the identifiability of the risk weighting assigned to each land cover with its percentage share of the catchment. Identifiability is quantified using the standard deviation of the optimum risk weighting for each land cover in each catchment. Plots are split to show results for: P (a and b) and N (c and d) for: high risk (a and c) and low risk (b and d) land covers.

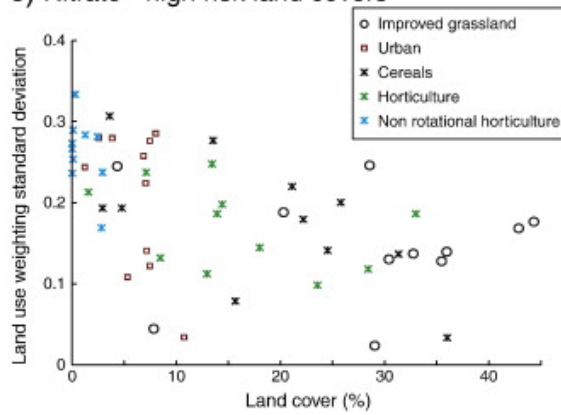
a) Orthophosphate - high risk land covers



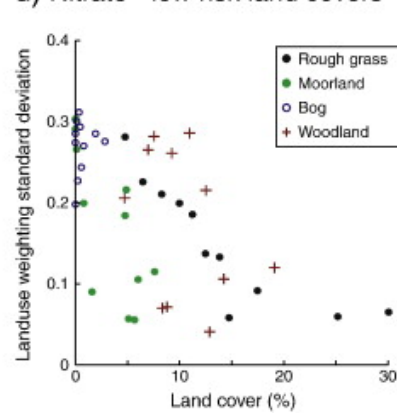
b) Orthophosphate - low risk land covers



c) Nitrate - high risk land covers



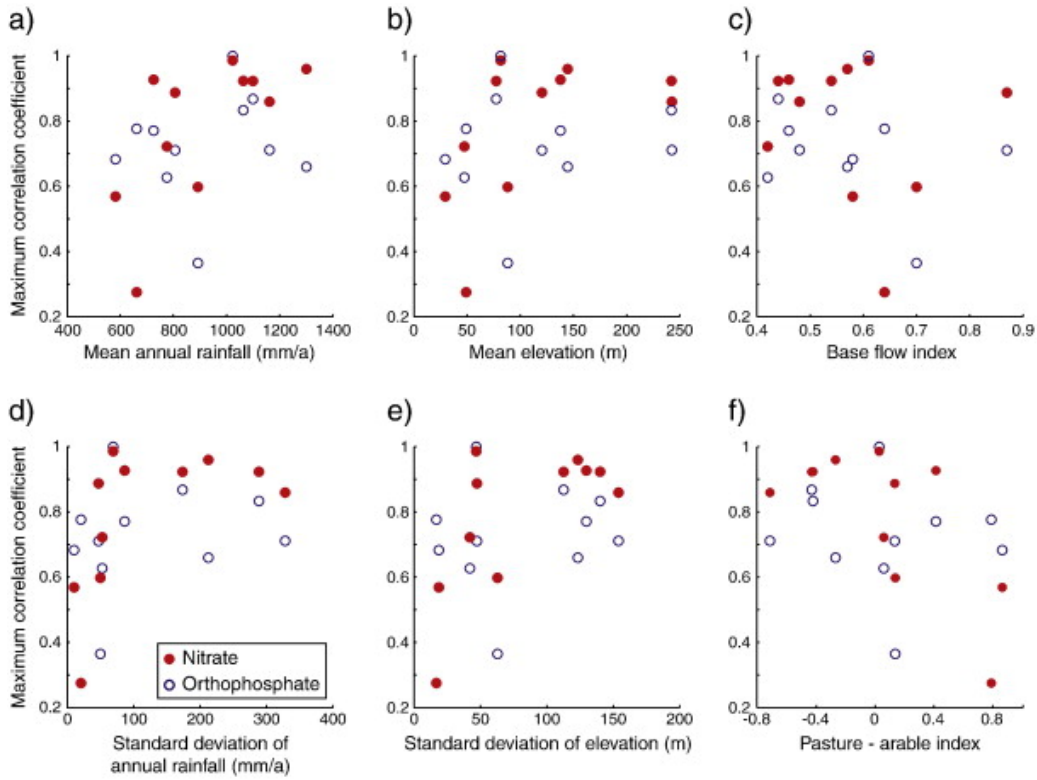
d) Nitrate - low risk land covers



086
087

088
089
090
091
092
093
094

Figure 5: Scatter plots showing the relationship between SCIMAP performance and catchment characteristics. Model performance is quantified using the correlation coefficient of predicted risk against GQA observations for the optimum SCIMAP run. The catchment characteristics are quantified through a set of metrics to represent mean and variability in annual rainfall (a and d); mean and variability in elevation (b and e); hydrological regime using the baseflow index (c) and catchment land use from the pasture arable index (f).

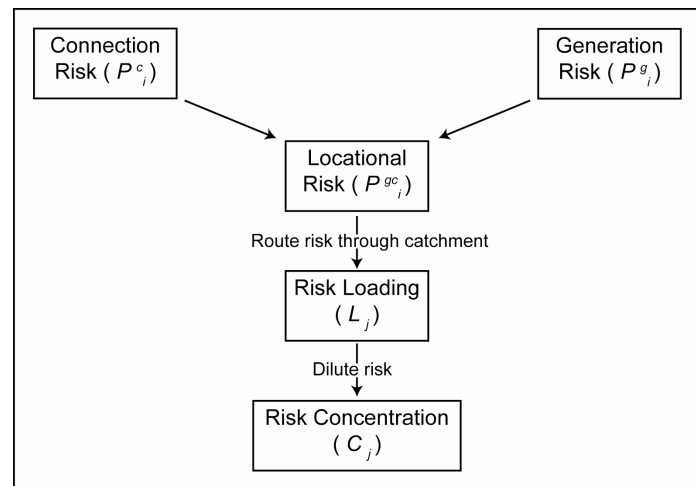


095
096
097

098 **Appendix 1: SCIMAP Model Structure**

099 Formulation of the model requires: 1) determination of the generation risk (p_i^g); 2) determination of the
 100 delivery index, or connection probability (p_i^c) for that entrained material; 3) convolution of (1) and (2) to
 101 get the locational risk (p_i^{gc}); 4) routing of the locational risk to determine a risk loading (L_j); and 5)
 102 transformation of the risk loading to a risk concentration (C_j). An overview of the processing steps for the
 103 generation of the risk map is shown in Figure 6.

104 **Figure 6: SCIMAP processing steps**



105

106 **Generation Risk**

107 Generation risk (p_i^g) is defined as the likelihood that a location (i) in the catchment can *generate* (g) risk.
 108 Our treatment of generation risk depends on whether the generation requires physical entrainment. We
 109 assume that generation risk (p_i^g) for P and N does not require physical entrainment, i.e. that these
 110 nutrients can be dissolved in water, as a result the generation risk is solely a factor of the availability (p_i^e)
 111 of the nutrient at location i and we can equate p_i^g with p_i^e .

112

Equation 1

113

$$p_i^g = p_i^e$$

114

115

116

117

118

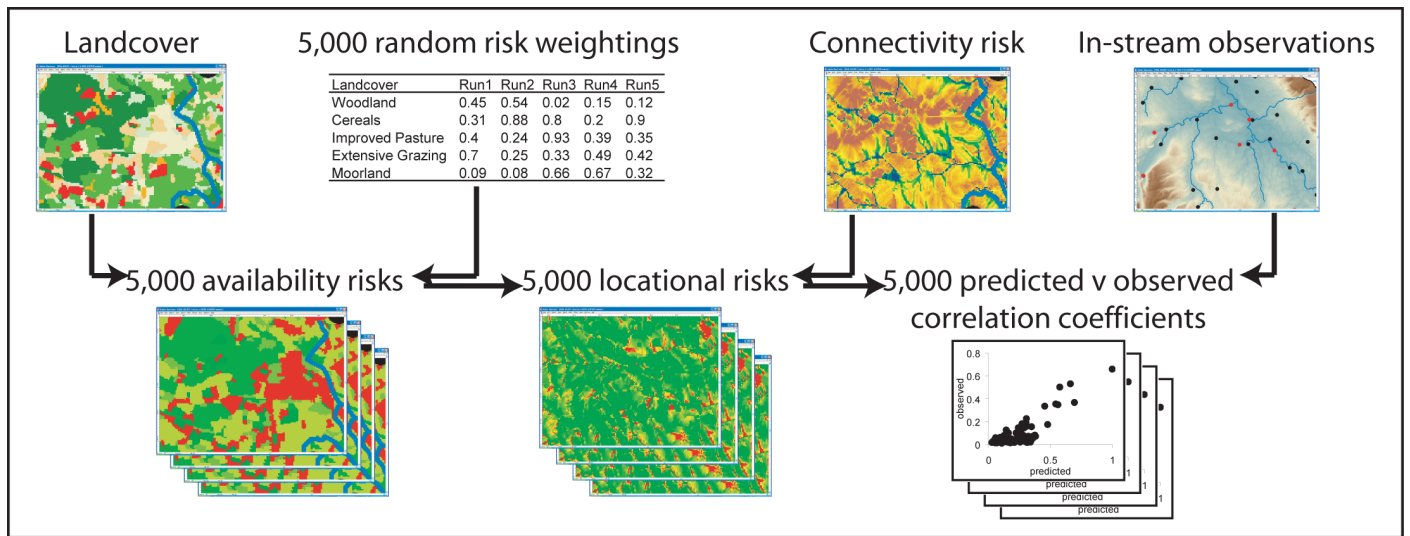
119

120

Availability (p_i^e) can be predicted using an inverse approach (Figure 7). We approach the inverse
 problem of unknown land cover risk weightings by using an uncertainty analysis (see below) to identify
 the values of p_i^e that best reproduce the spatial structure of distributed in-stream nutrient concentrations:
 i.e. we make no *a priori* assumptions about the p_i^e or its relationship with land cover. Instead we are
 matching SCIMAP predictions to in-stream nutrient observations in order to predict generation risk.
 There are two potential methods of achieving this: 1) an optimisation procedure based upon perturbation
 of the land use risk weightings to identify optimal set of risk values; or 2) a likelihood estimation

121 procedure (e.g. Beven and Binley, 1992) in which we identify the range of plausible land use risk
 122 weighting values. Both of these methods are with respect to independent validation data. We chose the
 123 latter as we were interested in the extent to which the delivery index treatment, coupled with the risk
 124 accumulation and dilution, yielded values that were logical with respect to what we know about the
 125 relationship between landuse and nutrient availability. We run 5000 model simulations, randomly
 126 selecting values in the range $0 \leq p^e_i \leq 1$ for each land cover for each simulation, i.e. with no *a priori*
 127 likelihood of any one land cover having a particular value of p^e_i . We determine an objective function to
 128 assess model performance appropriate to the nature of the validation data available for each simulation.
 129 In this case the selected objective function is the correlation coefficient from the relationship between
 130 predicted risk and observed nutrient concentrations.

131 **Figure 7: summary of the inverse modelling methodology**



132
133

134 **Connection Risk**

135 Our treatment of delivery or connection risk (p^c_i) has three primary assumptions. First, that rapid lateral
 136 surface or shallow subsurface flow is the dominant pathway for N and P delivery to the river network.
 137 The connectivity index represents disconnection associated with these processes provided that
 138 disconnection is controlled by a spatial distribution of soil moisture related to the condition where
 139 bedrock topography and surface topography have the same morphology. This is likely to be most valid
 140 for P, which is mostly sediment-bound (Walling et al., 1997; Withers et al., 1999), but also valid for some
 141 elements of the lateral flux of N, which can be transported in solution. Second, that the frequency and
 142 length of connected periods for each point in the landscape will be spatially structured, leading to a

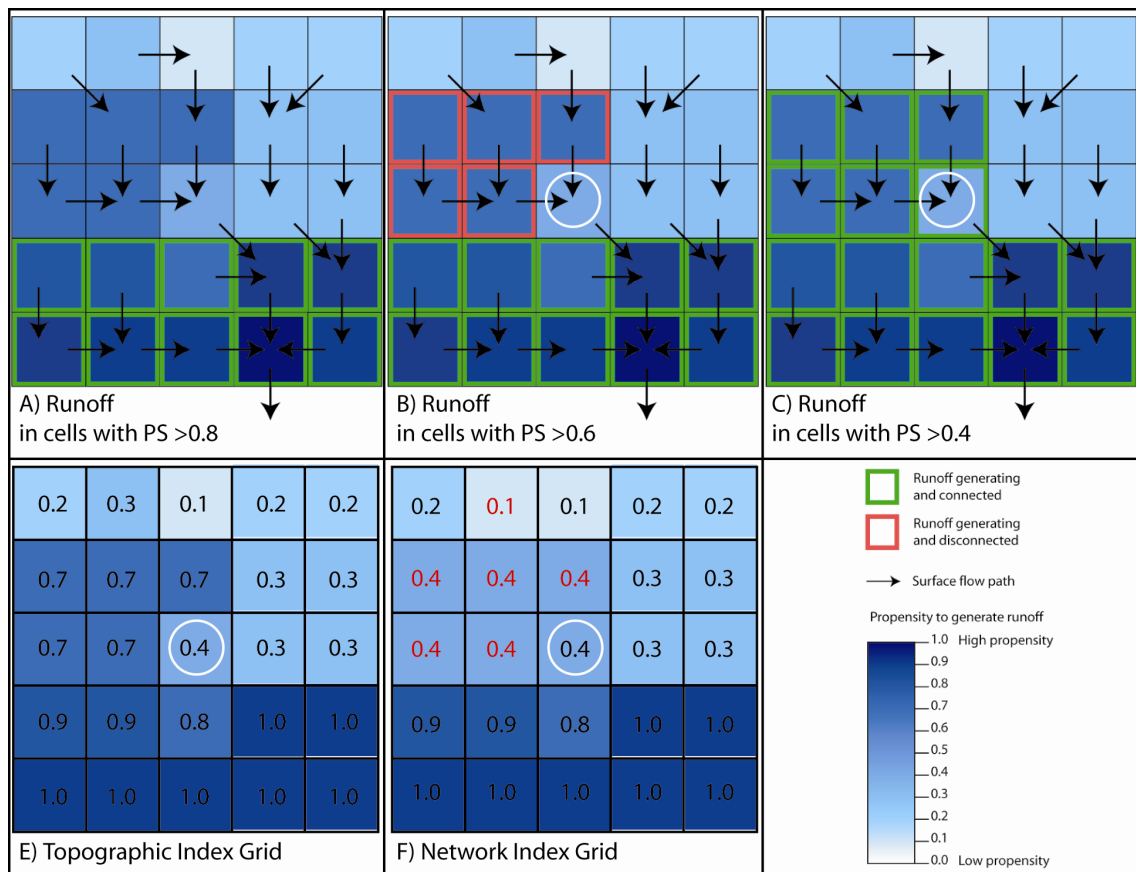
143 variable connection strength across the catchment. If we can find a reliable description of this spatial
144 structure then we can use it to determine the likelihood that generated material is delivered to the
145 drainage network. Third, that the topographic wetness index (Kirkby, 1975) can be used to describe
146 propensity to saturation and therefore the balance between lateral flux and vertical flux at a point. Flow
147 paths (from source to receiving water) where the soil columns are generally wetter *throughout* the flow
148 path, are more likely to be able to flux water, and hence material, laterally (Lane *et al.*, 2009). If we can
149 identify the point along the flow path where flux is most likely to be vertical, and quantify the extent to
150 which that is the case, we have a measure of the likelihood of disconnectedness, the inverse of which is
151 the propensity to connect. Here, we use the network index (Lane *et al.*, 2004) to determine this attribute:
152 this is the lowest value of the topographic index along the dominant flow path between a location in the
153 catchment and the river network. The topographic wetness index (TI) expresses the propensity to
154 saturation as the ratio of the upslope area per unit contour length (A) draining through a point in the
155 landscape and the tangent of the local slope (β), the latter assumed to represent the hydraulic gradient.

156 **Equation 2**

157
$$TI = \ln\left(\frac{A}{\tan \beta}\right)$$

158 Locations with a low value of the network index are assumed to have a particularly dry cell along their
159 flow path (Lane *et al.*, 2004), and hence are less likely to hydrologically connect, whether through
160 shallow subsurface flow or surface flow. We map the network index onto the probability of connection
161 (p^c_i) or delivery index using a distribution approach, scaling the network index between the 5th and 95th
162 percentiles and assigning risk values of zero and one at either end of this distribution.

163 **Figure 8: Schematic illustrating the Network index: Boxes A-C illustrate an example of cells on a**
 164 **hillslope generating runoff during a rainstorm. Early in the storm cells near the channel with a**
 165 **high propensity to saturation begin to generate runoff, these are connected to the river (green);**
 166 **later as more rain falls and the catchment becomes wetter a patch with a slightly lower**
 167 **propensity to saturation begins to generate runoff but these cells are not connected to the**
 168 **channel (red) because there is no continuous flow path of runoff generating cells connecting**
 169 **them with the channel. Finally the (white ringed) cell with a still lower propensity to saturation**
 170 **begins to generate runoff and at this point all the cells upslope of it that are generating runoff**
 171 **become connected to the channel (green). Boxes E and F show the differences between**
 172 **propensity to saturation as defined by the topographic index (E) and propensity to connection as**
 173 **defined by the network index (F). Note the red values in F which highlight cells where these two**
 174 **values differ, and the white ring which highlights the cell controlling connectivity in this case.**



175
176

177 Lane *et al.* (2009) compared the information on the spatial patterns of hydrological connectivity revealed
 178 by continuous simulation using a physically based, distributed hydrological model with the network index.
 179 They found that significant spatial variability in both the propensity to connection within a time period, as

180 well as the duration of that connectivity, can be explained using the network index. Although specifically
 181 formulated for surface overland flow, the analysis ought to apply equally for shallow subsurface flows
 182 and fluxes of material in terms of vertical versus lateral fluxes. They found that, locations with a higher
 183 Network Index are connected for longer, and the spatial signal of topographically induced wetness
 184 results in partial control of the dynamics of surface overland flow connectivity and potentially delivery.

185 **Locational risk**

186 We combine the generation and delivery risks to determine the locational risk of delivery of generated
 187 material to the drainage network (p_i^{gc}):

188 **Equation 3**
 189
$$p_i^{gc} = p_i^g \cdot p_i^c$$

190 **Routing, Accumulating and Dilution of locational risk**

191 We route and accumulate the locational risk under the assumption that this is driven by the
 192 topographically-driven accumulating area: i.e. the risk at a point is the sum of all locational risks
 193 upstream of that point. This leads to the risk loading to a point in the drainage network (L_j) with j upslope
 194 contributing cells that will increase monotonically with distance down through the drainage network:

195 **Equation 4**
 196
$$L_j = \sum_{i=1}^j p_i^g \cdot p_i^c$$

197 The risk loading takes no account of: 1) the propensity for dilution, where a high loading from a small
 198 upstream contributing area will have a more serious environmental effect than a high loading from a high
 199 upstream contributing area (e.g. Figure 2); or 2) loss of risk (e.g. due to deposition or chemical
 200 transformation). In this report, we assume that (2) is negligible. However, dilution is a critical property of
 201 drainage networks. The simplest way to deal with dilution is to scale the loading by the upslope
 202 contributing area to give a risk loading per unit area, akin to a concentration (C_j);

203 **Equation 5**
 204
$$C_j = \frac{\sum_{i=1}^j p_i^g \cdot p_i^c}{\sum_{i=1}^j a_i \cdot r_i}$$

205 where: a_i is the cell size and r_i is the rainfall weighting factor. This equation takes account of possible
 206 rainfall variations between sub catchments and the propensity for such variation will increase with basin
 207 size. This is represented by weighting upslope contributing areas by the amount of upstream contributed

208 precipitation, using temporal averages that reflect the time-integration of the study. However, such an
209 analysis is complicated by the fact that spatial variability in precipitation should also result in spatial
210 variability in connectivity. Hence, the predicted relative long term average wetness also utilises the
211 rainfall weighting factor.

212

213 **References**

214

215 Beven K, Binley A. The future of distributed models: model calibration and uncertainty prediction. *Hydrol*
216 *Process*, 1992; 6: 279-298.

217

218 Kirkby MJ. Hydrograph modelling strategies, in Reel R, editor, *Process in Physical and Human*
219 *Geography*, Heinemann, 1975, pp 69-90.

220

221 Lane SN, Brookes CJ, Kirkby MJ, Holden J. A network-index based version of TOPMODEL for use with
222 high-resolution digital topographic data, *Hydrol Process*, 2004, 18, 191-201.

223 Lane SN, Reaney SM, Heathwaite AL. Representation of landscape hydrological connectivity using a
224 topographically driven surface flow index. *Water Resour Res*, 2009; 45: W08423.

225 Walling DE, Webb BW Russel MA. Sediment-associated nutrient transport in UK rivers, in *Freshwater*
226 *Contamination*, in Webb BW, editor, Int Assoc Hydrol Sci, Gentbrugge, Belgium, 1997, pp 69–81.

227

228 Withers PJA, Dils RM, Hodgkinson RA. Transfer of phosphorus from small agricultural basins with
229 variable soil types and land use, in Heathwaite L, editor, *Impact of Land-Use Change on Nutrient Loads*
230 *from Diffuse Sources*, Int Assoc Hydrol Sci, Gentbrugge, Belgium, 1999, pp 41–50.

231

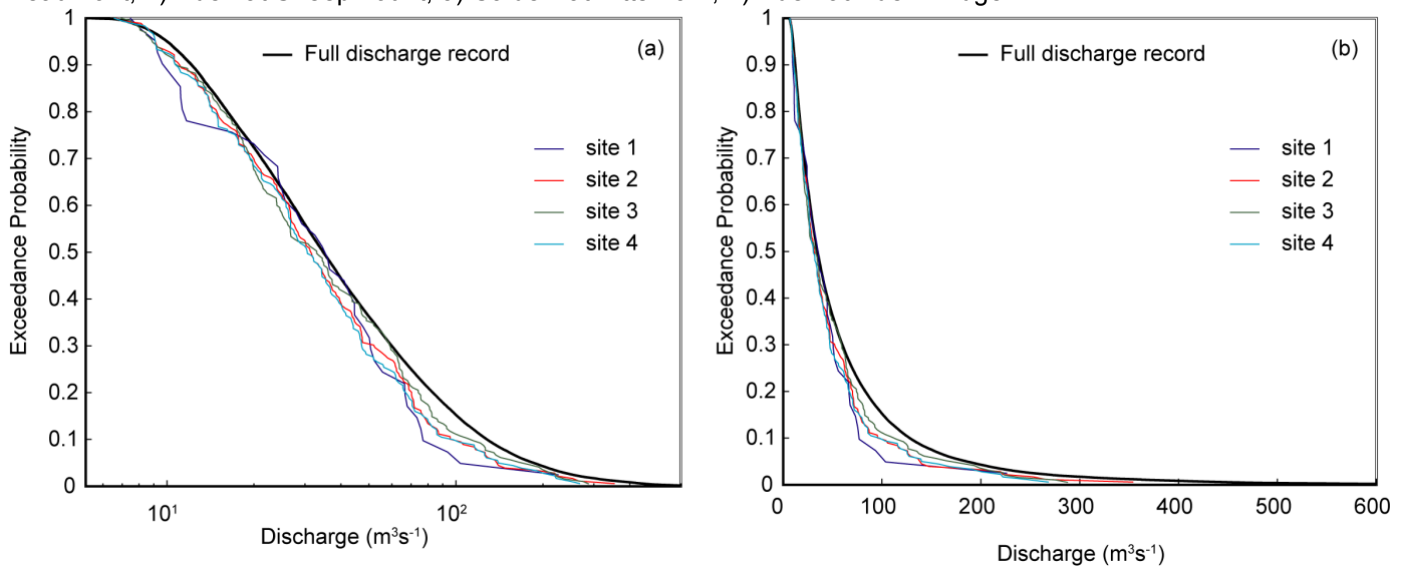
232

233 **Appendix 3: Testing suitability of simple means to integrate monthly N and P concentrations**

234
235 In this paper we use the mean of a set of concentration measurements as a time integrated measure of
236 relative risk. Our approach aims to make use of the GQA data which are imperfect but are the best
237 spatially distributed observations available. This approach has been used for the same environment
238 agency datasets at other UK sites (Davies and Neal, 2007; Rothwell et al., 2010). It assumes that the
239 monthly samples an adequately representative sample of instream nutrient concentrations to give the
240 relative magnitudes of the mean concentrations. We tested this assumption for the Eden catchment where
241 we had both concentration and discharge data. Our GQA data record was 15 years long from 1990 to
242 2005. The mean number of observations per site was 155 with a standard deviation of 38 observations.
243 We compared the distribution of flows over which concentration samples were collected with the full
244 distribution of flows to check for a low flow bias to our samples.
245

246 Figure 1 shows the results from our comparison of exceedance probabilities for only times that
247 concentration samples were collected and for the full record. The exceedance probability curves (Figure
248 1) suggest that concentration measurements were taken across a reasonable distribution of high and low
249 flows. On the basis of our results we suggest that the GQA data contain a large enough number of
250 samples over a long enough period to sample the range of flow conditions so that they do not suffer a
251 strong low flow bias. Flow weighting might improve the concentration estimates slightly but the number
252 of sites that could then be used would be limited by the availability of discharge data, which is even more
253 limited than concentration data in terms of spatial coverage. Since we are interested in the mean
254 concentrations as a time integrated measure of relative risk slight improvements in mean concentrations
255 are not worthwhile if they require significant reductions in spatial coverage.
256
257

258 Figure 9: Exceedance probabilities for discharge (on (a) a logarithmic scale and (b) a linear scale) for the Eden at
259 Sheepmount and for the discharges at which orthophosphate samples were collected from sites 1) Eden at
260 Beaumont; 2) Eden at Sheepmount; 3) Caldew at Bitts Park; 4) Eden at Eden Bridge.



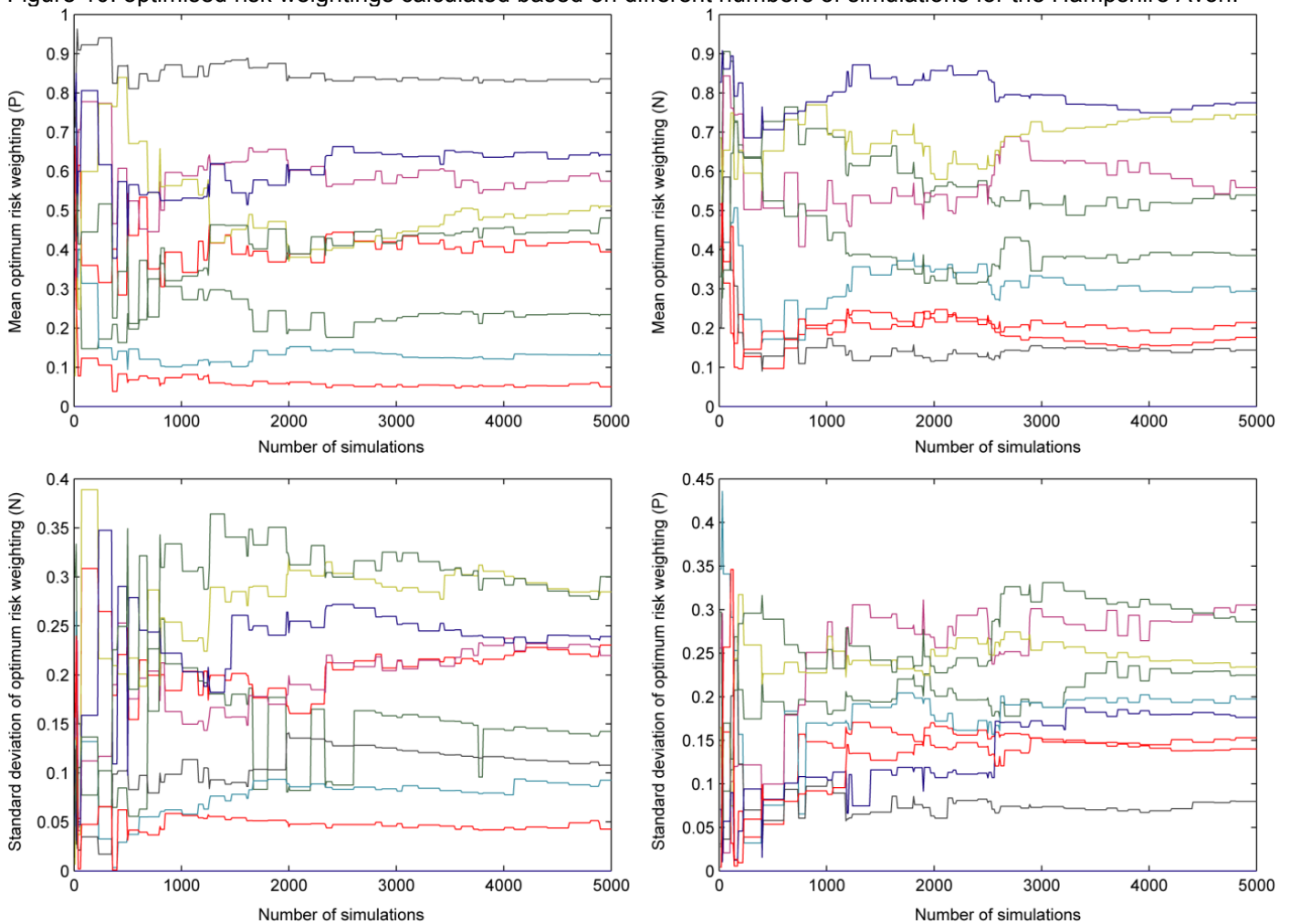
261
262
263
264

265
266
267
268
269
270
271
272
273
274
275
276
277
278
279
280
281
282

Appendix 3: Identifying the number of simulations required to sample the parameter space

We have tested the influence of the number of simulations for the Hampshire Avon catchment by calculating the optimum risk weightings using from 50 to 5000 simulations at 50 simulation increments. Our results suggest that the means and standard deviations become stable at around 2500 simulations and optimized means do not change their relative ranking beyond 3000 simulations (Figure 10). The optimized mean weights vary by <0.08 (or $<27\%$ of their average standard deviation) between 4000 and 5000 simulations and standard deviations vary by <0.04 (or $<20\%$ of their average value). There is a considerable reduction in this variability if considering only the high or low risks (significantly different from the null case at 90% confidence). For these land covers the optimized means vary by <0.04 (or $<16\%$ of their average standard deviation) between 4000 and 5000 simulations. These results suggested that 3000 simulations might be adequate to produce stable estimates and that 5000 simulations would include considerable redundancy. One of the reasons for the relatively low number of simulations required to identify stable values may be the distribution of land covers in our catchments. In each catchment some land covers have little or no coverage, reducing the number of dimensions for the parameter space and therefore the number of required simulations.

Figure 10: optimised risk weightings calculated based on different numbers of simulations for the Hampshire Avon.



283
284
285
286